

広島大学学術情報リポジトリ
Hiroshima University Institutional Repository

Title	MINERALOGICAL STUDY OF WEATHERING ON THE BANA COMPLEX, WESTERN PART OF CAMEROON
Author(s)	WOUATONG, ARMAND SYLVAIN LUDOVIC
Citation	Journal of science of the Hiroshima University. Series C, Earth and planetary sciences , 11 (1) : 55 - 99
Issue Date	1998-03-30
DOI	
Self DOI	10.15027/53162
URL	https://ir.lib.hiroshima-u.ac.jp/00053162
Right	
Relation	



MINERALOGICAL STUDY OF WEATHERING ON THE BANA COMPLEX, WESTERN PART OF CAMEROON

By

WOUATONG ARMAND SYLVAIN LUDOVIC

With 1 Table, 39 Text-figures and 8 Plates

(Received, February, 27, 1998)

ABSTRACT: The Bana complex is composed of various rocks from volcanics to plutonics located in the western part of Cameroon at latitude $5^{\circ}08'N$ and longitude $10^{\circ}20'E$. The climate of this region is essentially sudanese tropical type characterized by alternation of humid and arid seasons. The annual precipitation in this area amounts to 1500-2500mm. Under these circumstance, the Bana complex is extensively weathered. The basement rock is composed of gneiss (orthogneiss) which is intruded and covered by later plutonic rocks from gabbro to granite and volcanic rocks, from basalt to rhyolite, respectively. Many weathering profiles selected in the granite as well as in volcanic rocks were investigated in detail. Mineralogical characteristics such as chemical composition and micro-morphological variation of the weathering products were examined by means of X-ray diffraction (XRD), microprobe analysis (EPMA), X-ray fluorescent (XRF), scanning and transmission electron microscopy (SEM and TEM).

Halloysite and kaolinite are the most predominant weathering products regardless type of the host rocks. Detailed mineralogical investigation on the selected profiles revealed the transformation sequence of kaolin minerals as weathering proceed. That is, the lower parts are rich in halloysite whereas the upper parts are rich in kaolinite with a small amount of halloysite. The obtained mineralogical sequence was further confirmed by micro-morphological investigation of these minerals, i.e., from spherical halloysite to finally platy kaolinite.

Spherical halloysite associated with short tubular crystal is characteristic in the bottom part whereas irregular platy crystals predominate in the upper parts. These morphological variation together with crystal size reasonably explain the formation of kaolin minerals and crystallographical transformation sequence from spherical halloysite, short tubular halloysite, long tubular halloysite and finally platy kaolinite was established.

Etch pits developed on quartz and K-feldspar grains are commonly observed. However, shape and size of the etch pits are quite complicated suggesting none monotonous micro-weathering condition. Etch pits found in the upper part are much rougher than those of the lower part.

Based on the results obtained, weathering condition prevailed the Bana complex were discussed mainly from the stand point of clay mineralogy.

CONTENTS

- I. INTRODUCTION**
- II. GEOLOGICAL SETTING**
- III. SAMPLING AND EXPERIMENTAL METHODS**
- IV. EXPERIMENTAL RESULTS**
 - 1- X-RAY DIFFRACTION ANALYSIS**
 - 2- CHEMICAL ANALYSIS**
 - 3- SCANNING ELECTRON MICROSCOPY (SEM) OBSERVATION**
 - 4- MORPHOLOGY OF CLAY MINERALS**
- V. DISCUSSION**
- VI. CONCLUSION**
- REFERENCES**

I. INTRODUCTION

The Bana complex is composed of various igneous rocks from acidic to basic and from plutonic to volcanic rocks and is located in the western part of Cameroon at latitude $5^{\circ}08'N$ and longitude $10^{\circ}20'E$. The district is situated along the "Cameroon line" marked by about 60 alkaline anorogenic complexes aligned $N30^{\circ}E$ following the "Cameroon line" (Tchoua, 1974). The main volcanic activities have occurred along this lineament. The Bana complex is elliptical to ovoid in shape with 9 to 11 km long and 5 to 7 km wide, covering about 50km^2 . Three main peaks are identified in the district, Batchingou 2097m, Lembo 2045m and Bana (ss) 2042m. The highlands of this region are characterized by a series of stepped plateaux dominated by large volcanic highland and depressed basin (Morin, 1980). The climate of this region is essentially that of the Sudanese tropical type characterized by its contrasted seasons, i.e., four months of dry season from middle November to middle March and eight months of raining season with most abundant rainfall in August, September and October. The annual precipitation is estimated at 2500 to 3500mm of rainfall per year (Siffermann and Millot, 1969). The hydrography is dendritic type characterized by their permanent rising during the year. Numerous rivers and streams rise from the region covered by basaltic lava flow, trachytic and rhyolitic slab, developed in the highland and the fact is intimately related to natural disasters occurred in the district. The topography of the district is characterized by pyramid stages with different vegetations (Tchawa, 1991). In general the vegetation is typically that of the grassland region of western Cameroon characterized by herbaceous savana with thorn shrub and the vegetation is related to weathering degree of the Bana complex. Extensive weathering even produces several clay deposits in the region.

Dumort (1968) reported the first geological map of the district and revealed that the Bana complex is composed of alkali granitic pluton associated with rhyolitic tuff. He proposed the following geological sequence.

- Intense mylonitization of a basement zone;
- Ending of volcanic activity by an explosive rhyolitic phase;
- Intrusion of granitic batholith;
- Intense hydrothermal alteration related to the late granitic activities. Subsequently Tchoua (1974) noticed the presence of gabbroic rocks on the eastern flank of the complex. Lasserre (1978) dated by Rb-Sr method using biotite in the Batcha granite at 30 Ma. Nana (1988) reported that the Bana complex is an anorogenic complex saturated in silica comprising volcanic and plutonic rocks and that the volcanic series has intermediated nature between basalt and rhyolite. He dated by K-Ar method the age of volcanics at about 40 Ma. The associated plutonic series includes leucogabbro, monzodiorite, monzonite and granite. Caen *et al.*, (1991) dated the granitic rocks (Lembo granite) at 51 Ma. Area photos on the scale of 1/50000 obtained from the National Institute of Cartography Yaounde Cameroon show preferential lineaments around the Bana complex (Nana, 1988; Tchawa, 1991). As is evident in (Fig. 1) two predominant directions are recognizable, one is $N50^{\circ}-60^{\circ}$

E and the other $N65^{\circ}-85^{\circ}E$ and the former is called Somalian trend and the later Adamaoua trend (Tchoua, 1974). Additional subdirections such as $N30^{\circ}-40^{\circ}E$ (Cameroon line), $N45^{\circ}-50^{\circ}W$ (the Erythrean trend) and N-S (the panafrikan chain) are recognized. The rocks of the district, the Bana complex are characterized by severe weathering. The rocks are attacked extensively by water, oxygen, and carbon dioxide and the reactions proceed spontaneously under the tropical climate. Alteration by weathering is the expression of the constituent minerals of the igneous rocks adjusting to the equilibrium of the surface conditions.

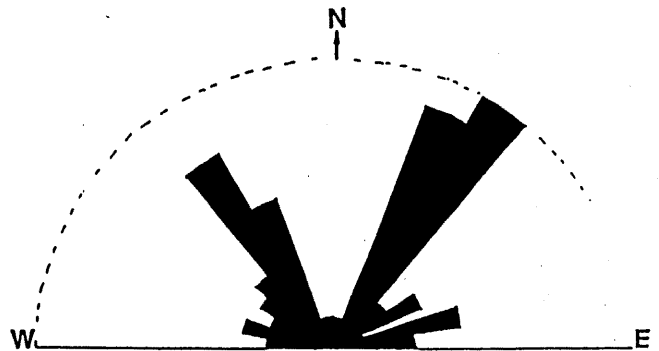


Fig.1 Rose diagram of lineaments of the Bana region.

Intimate relationship between weathering and clay minerals have been studied by many investigators (e.g. Anand *et al.*, 1985; Bird *et al.*, 1990). It has been established that halloysite is first formed and transformed to kaolinite during weathering process of granitic rocks under temperate climate as well as under tropical condition (Parham, 1969; Nagasawa and Kunieda, 1970; Kitagawa and Kakitani, 1977; Tazaki, 1981). Moreover, morphology of halloysite and kaolinite varies complicatedly depending on the weathering condition and also on the rock type (Nagasawa, 1969; Nagasawa and Miyazaki, 1975; Keller, 1989). In addition kaolin minerals are also commonly formed by hydrothermal alteration and even by diagenesis. However, detailed mechanism and/or transformation process of the clay minerals have not been established up to the present. In other words, precise and/or micro-environmental conditions controlling the transformation of clay minerals together with morphological variation are remained to be solved. In relation to weathering, observation of etch pits found on the surface of relatively resistant minerals such as quartz and K-feldspar provides significant information

concerning alteration condition (Kitagawa *et al.*, 1994). The Bana complex provides great possibility to clarify the mineralogical alteration process since abundant and various clay minerals are formed under the humid and arid tropical conditions.

In the present paper, weathering process of the Bana complex is examined based on the mineralogical stand point. Special attention will be paid on the variation and transformation of clay minerals as well as on their micro-morphology. Etch pits developed on the grain surfaces of quartz and K-feldspar collected from the weathered rocks will be also examined in detail.

ACKNOWLEDGEMENTS

The author wishes to express his sincerest gratitude and appreciation to professor Setsuo Takeno and Associate professor Ryuji Kitagawa of the Hiroshima University, to professor Tchoua M Felix and Associate professor Njopwouo Daniel of the Yaounde I University for their enthusiastic guidance, encouragement, valuable criticisms and advice throughout the progress of the present work and during his stay in Japan. He is also greatly indebted to professors Yuji Sano, Satoru Honda, Toru Takeshita of the Hiroshima University for their critical reading on the manuscripts. Drs Yasutaka Hayasaka, Makio Ohkawa and Mr Asao Minami, who helped in computer calculations to determine the chemical composition and technical assistance in using laboratory facilities, are thankfully acknowledged.

Sincere thanks are extended to Dr Nkonguim Nsifa Emmanuel for their kind guidance during field works and to all the staff of the Department of geology, University of Yaounde I for their helpful advice and kind assistances.

Special thanks are also due to Japanese Government's, Ministry of Education, for his financial support for 3 years 6 months.

I wish to thank my family and family-in-law for taking good care of my children during my stay in Japan. To my late father who died in October 1995, may your soul rest in peace.

Finally, the author would like to express heart-deep appreciation to Mrs Wouatong Yvonne, his wife, Gaelle his daughter, Cyrille and Landry his son, for their understanding in the present work and struggles in daily life while he was away from them for a long time.

II. GEOLOGICAL SETTING

1- Basement rocks

The basement rocks of the Bana complex is composed of gneissose rocks such as orthogneiss and porphyroid granite. The former is developed mainly in the northwestern part of the district (Fig. 2). The orthogneiss is intruded by dykes such as trachytic rocks and covered by pyroclastic sediments. Clear alternate bands of dark thin layer rich in ferromagnesian minerals and those rich in quartz and feldspar are developed.

The porphyroid granite is grayish coarse grained rock containing feldspar megacryst arranged in certain directions. The geological age of the basement rocks have not been established yet. However, relative relation to the granitic rocks the formation age can be said older than Mesozoic.

2- Plutonic rocks

In the Bana complex, syenite and granitic rocks such as Lembo, Batchingou and Batcha granite are developed from the north to the south ends of the district (Fig. 2). The ages of these plutonic rocks are 30 Ma for Batcha granite (Lasserre, 1978), 51 Ma for Lembo granite (Caen *et al.*, 1991).

- Quartz syenite

Syenite is developed mainly in the northern part of the district. The rock is medium to fine-grained and greyish in colour. The main constituent minerals are quartz, K-feldspar, plagioclase and biotite. Sphene, apatite and secondary calcite are also present as accessory minerals. Plagioclases (20% in volume of rock) are andesine (38-43% An) and oligoclase (16-25% An). They are anhedral to subhedral and (3-4mm) in size surrounded by K-feldspar showing the symplectic intergrowth. K-feldspar reaches almost 50% of volume and is subhedral to euhedral with composition of 70-98% Or and 6-8mm × 3-5mm in size. Amphiboles (10% in volume) are mostly ferro-hornblende. They occur as subhedral flakes with (4 × 2mm) in size, and show light greenish in colour. Some amphibole contain calcite often associated with oxide. Biotite is less than 5% in volume and occurs as anhedral flakes (3 × 1mm), and is replaced commonly by calcite. Quartz, 15% in volume is mostly anhedral and varying from 3mm to less than 1mm in size. Secondary quartz is also common associated with calcite. Pyroxenes are very few and rare. They are augite and ferro-augite occurring as very discrete anhedral grains associated intimately with amphibole. Oxides are mostly ilmenite and occur as inclusion in amphibole. Accessory minerals such as sphene, zircon, apatite and chlorite are rather common.

- Lembo granite

In the northeastern part of the district, granite characterized by K-feldspar and aegirine is distributed widely (Fig. 2). The Lembo granite is coarse grained and grayish in colour. K-feldspar is 8-6 × 3mm in size and is anhedral to subhedral. The mineral is essentially orthoclase and the volume of K-feldspar reaches almost 60% of the rocks. Plagioclases rarely occur albite mantled by alkali feldspars. It is anhedral less developed than alkali feldspar. Amphibole 8.5% in volume is ferroeckermannite, occurs as large (up to 0.5cm) poikilitic crystals enclosing aegirine. The mineral shows strong pleochroism, deep prussian blue (Np) to brownish green (Nm) colour and low birefringence. Twin is rare and altered partially to biotite. Biotite is small in amount occupying 6.5% in volume and occurs as pale brown flakes in amphibole and contains occasionally zircon as inclusion. Pyroxene ferro-augite, is observed in some samples and the volume is about 2%. The crystal is subhedral less than 3mm in size with very weak pleochroism (greenish yellow on Ng and pale yellow on Np). Symplectic association with quartz is sometimes observable. Quartz more than 18% in volume is subhedral to euhedral and shows symplectic association

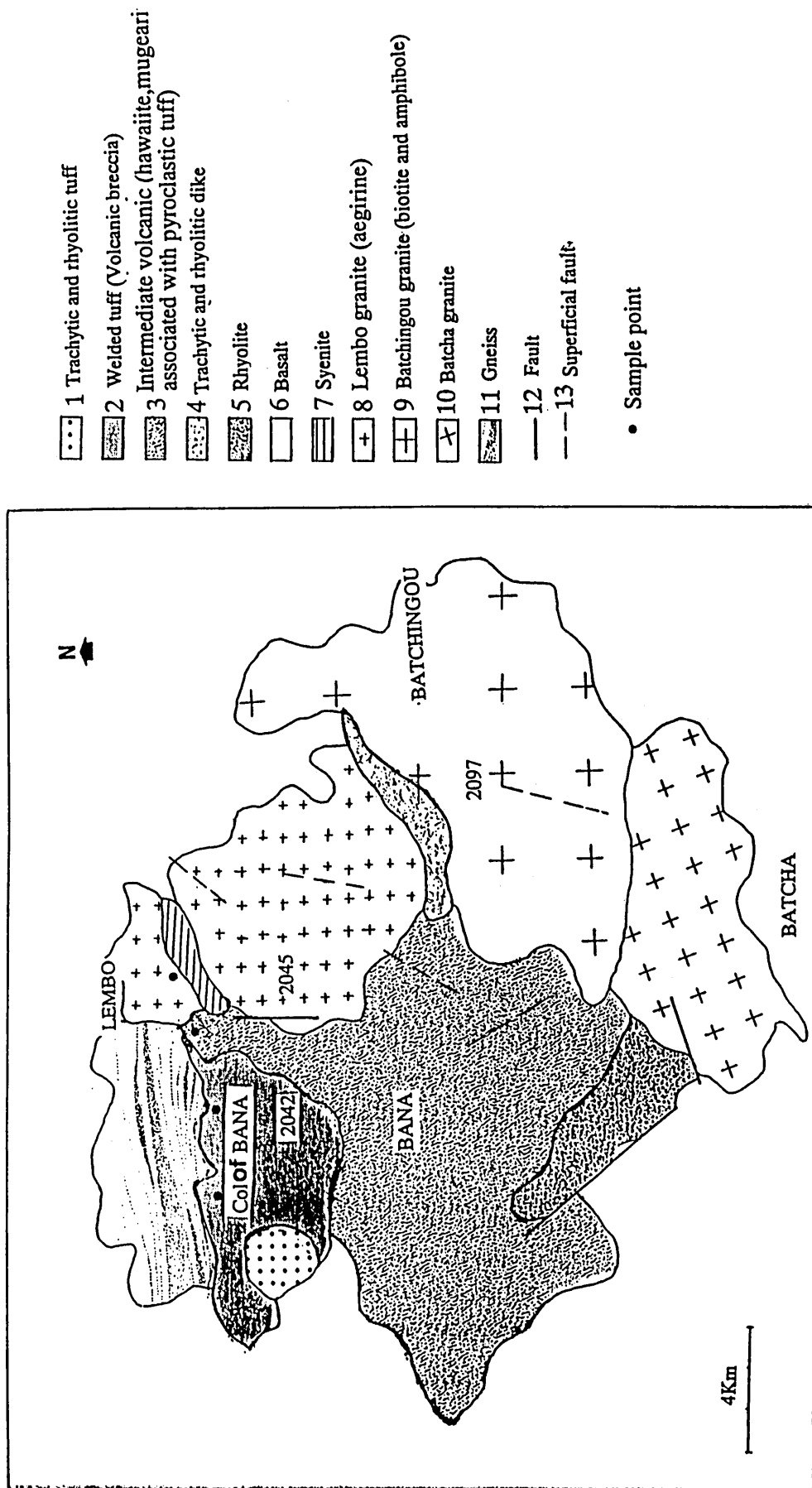


Fig.2 Geological map of the Bana complex.

with K-feldspar. Apatite zircon, chlorite, sericite and damourite are also present.

- Batchingou granite

In the middle eastern part of the district, medium to fine grained granite is distributed widely (Fig. 2). The medium grained granite is found in the central to western part of the district (including the summit of 2097m) whereas fine grained is found mainly in the south eastern part. Nana (1988) confirmed extension of the pluton as 4km × 2km wide. The rock is composed of quartz, feldspar, amphibole and small amount of biotite. Epidote and zircon are present as accessories. Plagioclase 1% in volume is anhedral to subhedral, varying in size 6-2 × 3-1mm and the composition is between oligoclase and albite. K-feldspar (70% in volume) is essentially orthoclase (95-98% Or) and anhedral to subhedral varying in size forming often symplectic texture with quartz. Quartz is second abundant leucocratic mineral (25% in volume) and anhedral to subhedral. Amphibole (3% in volume) is ferro-edenitic hornblende and anhedral to subhedral. Biotite is contained in very small amount (0.8%) and is skeletal flakes with brownish colour. Chloritization is commonly observed. Opaque minerals are mainly ilmenite (0.2% in volume). They occur as rectangular to triangular form associated often with amphibole and biotite.

- Batcha granite

This granite is similar to Batchingou granite in constituent minerals but is characterized by granophyric textures. The rock distributes in the southern most part of

the district. Nana (1988) confirmed that the Batcha granite is older than Batchingou granite based on his field observation. K-feldspar (75% in volume) is essentially orthoclase and is subhedral to euhedral with 2-3mm in dimension. Some large crystals show a radial arrangement at their margins. Quartz (3% in volume) appears as anhedral form associated often with K-feldspar. Two types of intergrowth of quartz and orthoclase are identified: the micrographic type and the radial arrangement. Biotite (1% in volume) occurs as skeletal flakes and mostly associated with oxides. Apatite is included in quartz and K-feldspar. Zircon, sphene and epidote are recognizable.

In addition to the above mentioned granites, dolerite, monzonite and monzogranite are also present as small plutons in the Bana complex. Monzonite occurs as xenolith in the Lembo granite. Nana (1988) found it as xenolith in the Batchingou granite. Monzogranite outcrops as small pluton in the northeastern part of the complex. It is not mentioned in (Fig. 2) because of its little dimension. In Fig. 3 variation of the constituent minerals of the plutonic rocks found in the Bana complex is present.

3- volcanic rocks

In the Bana complex, various types of volcanic rocks are included. According to Tchoua (1974), these volcanic rocks are formed by fissural volcanism.

- Alkali basalts

Basaltic rocks are widely distributed surrounding the Bana complex in western Cameroon (Geze, 1941 and 1943; Tchoua, 1974; Gouhier *et al.*, 1974). The basaltic rocks are grayish black to dark gray in colour with a thin weathered layer (1-3mm) near the surface. Microlite porphyritic, microlitic seriated to aphyric textures are common accompanying tiny or needle-like crystals of olivine. Olivine and plagioclase are the main phenocrysts. Pyroxene phenocryst is also present. Olivine (41% in volume) is 80-83% fosterite in composition and occurs as phenocrysts, microphenocrysts and microcrysts. Crystal size is about 5.5 to 6mm and varies subhedral to euhedral in form. Iddingsitized rims are common and complete iddingsitization is also observable. Pyroxene occurs as phenocrysts and microcrysts (30% in volume). It is augite (41-42% Wo) in composition and is subhedral to euhedral, characterized by concentric zoning and lamellar twinning. Plagioclases are bytownite (71-69% An) and labrador (65-57% An) and occupy 25% in volume. They occur as randomly oriented microlite laths with albite twinning. Small inclusion of oxide and pyroxene blebs are occasionally observed. Opaque minerals are ilmenite and magnetite occurred as inclusion in pyroxene and plagioclase. The groundmass is composed of fine plagioclase laths, blebs of clinopyroxene, olivine grains (usually altered to iddingsite) and oxide. Calcite and zeolite together with quartz are found in vesicles.

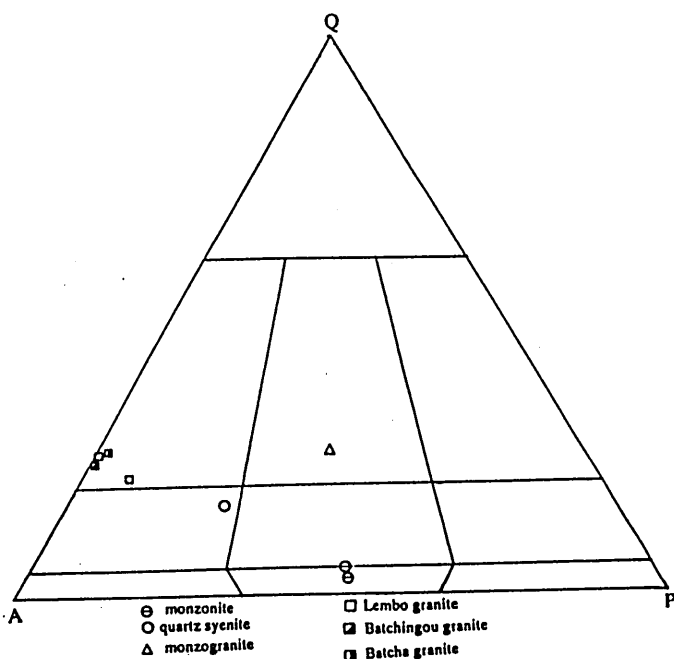


Fig.3 Q-A-P diagram of the plutonic rocks found in the Bana complex.

- Hawaiiite

This rock is found in the intermediate volcanics associated with welded tuffs and is developed in the western part of the district associated with welded tuffs, especially near the volcanic cones (Fig. 2). The rock is dark gray and contained plagioclase phenocrysts. Composition of plagioclases vary from bytownite (73-72% An), labrador (69-60% An) to andesine (56% An) and occupy 74.9% in volume. The crystals are anhedral to subhedral and the maximum size reaches 10mm long. Carlsbad twin bathing in a holocrystalline microlitic matrix is common. Phenocrysts and microlites are arranged in certain direction. Most plagioclase phenocrysts have core composition between 73 and 69% An and are normally zoned from the core to the rims. Oscillatory zoning is occasionally observed. Plagioclase microlites are labrador (57% An) and andesine (46% An). Pyroxenes (8% in volume) vary from salite (48% Wo) to augite (46% Wo). They are subhedral to euhedral with prism form (3 × 2-4 × 1mm) and show high interference colour and low pleochroism. Scattered pyroxene microcrysts in groundmass are either salite or augite. Olivine (3.4% in volume) is fosterite in composition (85-68%) and occurs as microphenocrysts or microcrysts. The mineral is corroded and cracked and is associated sometimes with calcite along the cracks. Oxide is anhedral ilmenite, often elongated along with plagioclase microlites and intergrowths with augite phenocrysts. Groundmass contains abundant plagioclase together with ilmenite, microlites olivine, salite and augite. Interstitial glass is rarely present.

- Mugearite and benmoreite

The rocks are found in the transitional region between basalt and trachyte in the intermediate product (Fig. 2). The rocks are grayish to gray in colour and have glomerocrysts of plagioclase and pyroxene showing microlitic and glomeroporphyritic texture. Plagioclase occurs as phenocrysts and microlites. The phenocrysts are anhedral to subhedral and labrador in composition (63% An). Pyroxenes often occur as microphenocrysts with augite composition (36-43% Wo). They occur as either glomerocrysts or scattered in groundmass. Ilmenite is anhedral and occurs associated intimately with augite. The groundmass contains abundant microlites of andesine (46% An) together with K-feldspar, augite, ilmenite and olivine. Glass is present in small amount.

- Trachyte

The rock occurred as dome associated intimately with rhyolite. It also intruded in the Batchingou granite and gneiss as dike. Trachytic tuff is also present. The trachyte is compact and mostly grayish in colour. Porphyrocrysts of K-feldspar and plagioclase are characteristic. K-feldspar (12% in volume) is sanidine (43-45% Or) in composition and anhedral to subhedral with (7-9mm) to (4-5mm) in size. Carlsbad twinning is common. Plagioclase (4% in volume) is oligoclase to albite (16-3% An) in composition and anhedral to subhedral. Both K-feldspar and plagioclase show alteration rim. The groundmass is composed mostly albite and shows trachytic texture together with augite, aegirine, hornblende, and ilmenite.

- Rhyolite

Rhyolite occurs as dome at the southwestern flank between Bana and Batcha, and between the Lembo and Batchingou granite. Lava flows and dikes in granite and volcanic breccia are also common. The rock is compact, light, brownish to greenish in colour. Two types are distinguished: one shows glomeroporphyritic microlitic texture accompanied with porphyritic K-feldspar and plagioclase. The other contains abundant needles of greenish pyroxenes and the matrix is constituted only of K-feldspar. K-feldspar (4.5% in volume) is anorthoclase (33-35% Or) in composition and subhedral to euhedral. The mineral occurs as glomerophytic and isolated microcrystals. Plagioclase (0.6% in volume) is albite (8% An) in composition and anhedral to subhedral tablets (2 × 1mm). Albite and/or pericline twin is common. The groundmass mostly glassy and microcrystalline is composed of plagioclase, quartz and ilmenite. Biotite and amphibole are rarely contained. Spherulitic texture composed of greenish pyroxene needles (70-80% in volume) is observable. In such case groundmass is essentially constituted of orthoclase (88-98% Or), quartz and oxide. Very fine intergrown needles of quartz and K-feldspar radiating from a common center are also present.

- volcanic breccia and volcanic tuffs

Distinction of the two rock types is rather difficult because of the deep weathering. The two types of rock are widespread on the northeastern part of the Bana complex. They distribute in a relatively narrow zone of 2 to 3km length over 500m to 1Km wide. These volcanics are often intruded by columnar basalt and by trachytic dikes. The intruded dikes are in general weathered more extensively than the host volcanic rocks. The breccia and the tuffs are dark gray to gray in colour and extremely welded. Lithic fragments and xenoliths are common. They are mostly fine to coarse grained showing eutaxitic texture. Blocks and fragmental materials are often oriented along the flowing direction. Weathered part of these welded tuffs is clearly recognizable by their colour such as whitish, yellowish, grayish and brownish. In the case of extremely welded, original porous pumiceous lapillis tuff changes to dense rock causing more resistivity against weathering. Blocks are consist of volcanic, plutonic and metamorphic rocks whose size varies from 1cm to more than 10cm in various forms such as angular and rounded. All these volcanic rocks have almost the same petrographic feature to those previously described. However, presence of coarse grains of carbonate, granite and gneiss are characteristic.

- Pyroclastic deposits

Two types of pyroclastic deposits are recognized in the intermediate volcanics, one is fall deposit and the other is flow deposit. The Bana pyroclastic deposits correspond to the flow type and distribute only in a small area. They are not stably emplaced and have great possibility to move because of the geographical characteristic of the district. Various size of blocs such as basalt, trachyte and rhyolite are contained in the deposit. Fig. 4 shows chemical characteristics of the volcanic rocks found in the Bana complex.

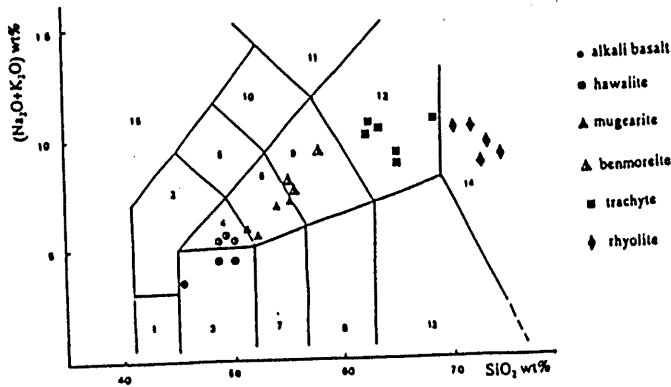


Fig.4 Variation of alkalin contents of the volcanic rocks found in the Bana complex against silica content. Classification of the rocks is taken from Le Bas *et al.*, (1986)

III. SAMPLING AND EXPERIMENTAL METHODS

The host rocks composed of the Bana complex such as granites, basalts, trachytes and rhyolites are collected together with those of weathered rocks. In addition to these samples, clay samples were taken from weathered profiles exposed recently by road cutting between Lembo and Bapou villages. Three main profiles in the Lembo granite, basic and acid volcanic rocks were investigated in detail. The profile of the Lembo granite is situated at the place of 1500-2000m in altitude, about 150-200m in width and about 25-35m in height. The most upper part of the profiles is covered with reddish soil of about 2-5m thickness (laterite soil). Profiles selected in the Lembo granite, 7 specimens were carefully collected from the lower to the upper parts of the granite. Profiles selected in the basalt (5 specimens) and rhyolite (5 specimens) were also examined.

Identification of the constituent minerals in the bulk samples and also clay fractions were determined by X-ray diffraction (XRD) method (Mac science-MXP 18 KVA). Detailed identification of clay minerals were performed after the following two treatments: 1) Untreated air dry condition; 2) treatment with formamide for a few hours (Churchman *et al.*, 1984 and Theng *et al.*, 1984).

Chemical composition of the major constituent minerals were examined by electronic microprobe (JCAM 733II superprobe). Analytical conditions are:- sample current 10mA; - acceleration voltage:15kv; - analytical time 6s per group of 3 elements; - size of beam 1-5 micron.

The bulk chemical composition of the host rock and weathered products were determined by X-ray fluorescence spectrometer (XRF) (Rigaku3030) equipped with a W dual anode X-ray tube. The obtained values

were calculated and expressed in the form of oxide. Measured elements are Si, Al, Ti, Fe, Mn, Mg, Ca, Na, K, Nb, Zr, Y, Sr, Rb, Th, Pb, Zn, Cu and Ni.

Quartz and K-feldspar were picked up from the specimens collected from weathered granite and acid volcanic rocks under the binocular microscope. Microtextures developed on the surface of the obtained grains were observed by scanning electron microscope (SEM) (Akashi-Alpha 10).

The characteristic micro-morphologies of clay fraction were observed both by transmission and scanning electron microscope (TEM:Jeol 200CX; and SEM: Akashi-Alpha 10).

IV. EXPERIMENTAL RESULTS

1 X-RAY DIFFRACTION (XRD)

The representative XRD patterns of the bulk and the clay fraction collected from the Bana complex are presented in Figs. 5, 6 and 7. These XRD show that the major constituent minerals are quartz, feldspar, goethite, gibbsite and kaolin mineral in all collected samples. After formamide treatment of the clay fraction, refraction at about 7Å shifts to about 10Å (Figs. 5B, 6B and 7B). According to Churchman *et al.*, (1984) and Theng *et al.*, (1984), halloysite if present gives shift to 10.4Å, whereas kaolinite does not expand beyond 7.2Å. The present result indicates that both halloysite and kaolinite are contained in each sample. Semi quantitative analyses using the reflection intensities normalized to 100% give us relative abundance of the constituent minerals in weathered granite, weathered basic volcanic rocks and weathered acid volcanic rocks (Figs. 5A, 6A and 7A).

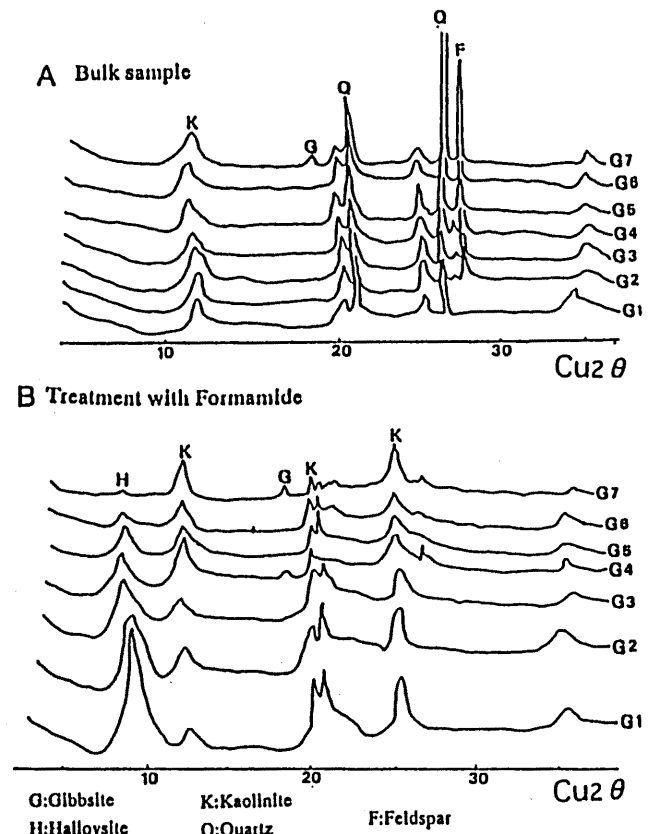


Fig.5 XRD pattern of clay fractions collected from weathered granite.

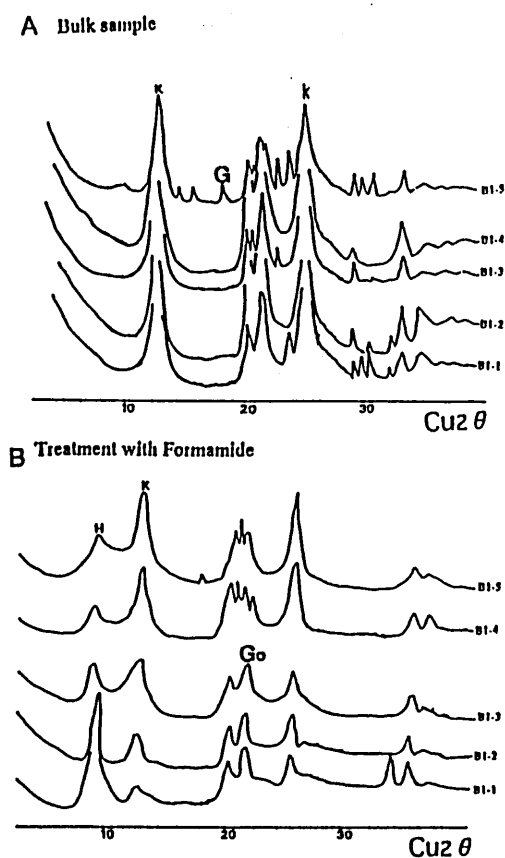


Fig.6 XRD patterns of clay fractions collected from weathered basic volcanic rocks.

G:Gibbsite K:Kaolinite F:Feldspar
 H:Halloysite Go:Goethite

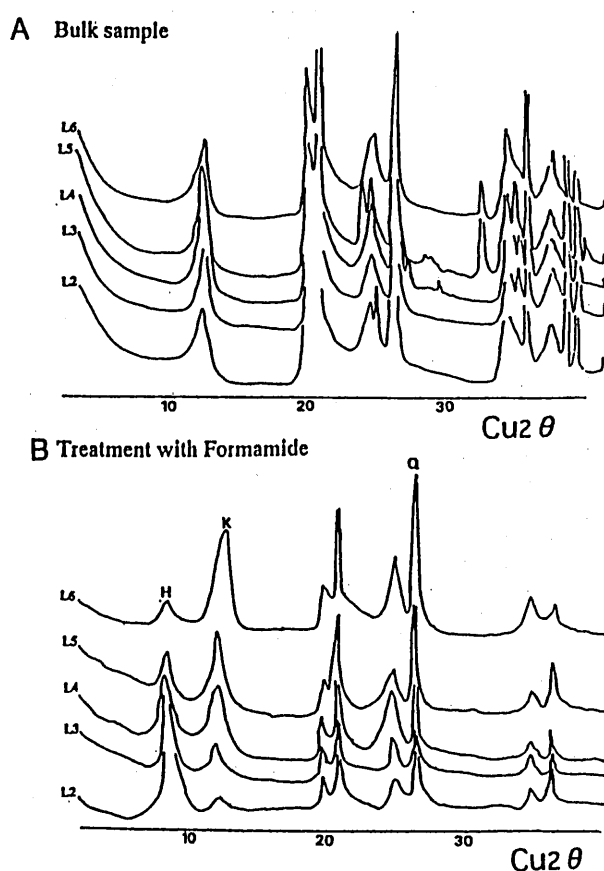


Fig.7 XRD pattern of clay collected from weathered acid volcanic rocks.

H:Halloysite Q:Quartz
 K:Kaolinite

respectively). Fig. 8 shows the variation of relative abundance of the constituent minerals in the bulk samples (Fig. 8A) and in the clay fractions (Fig. 8B) as a function of depth. Quartz and feldspar contents decrease with increasing of depth. Halloysite increases with depth while kaolinite decreases with depth (Fig. 8B). As seen in Figs. 9A and 9B, quartz content tends to decrease with depth in weathered basic volcanic rocks, whereas that in weathered acid volcanic rocks increases with depth. Content of kaolin minerals shows the same variation to those of weathered granite. Clay fractions (less than $2\mu\text{m}$) is generally considered to be the product of weathering (Calvert *et al.*, 1980). Halloysite (10.4\AA) is believed to appear as an early product of weathering than kaolinite. It can be confirmed that the constituent minerals commonly change from the lower part to the upper part in the vertical direction.

As is clear in Figs. 5, 6 and 7, samples collected from the lower parts contain more halloysite associated with small amount of kaolinite than those of the upper parts.

2. CHEMICAL ANALYSIS

Detailed chemical composition of the constituent minerals contained in various rocks found in the Bana complex was determined by electron microprobe analyses. The bulk chemical composition of the rocks of the Bana complex were measured by X-ray fluorescent method. In the measurements, trace elements such as Nb, Zr, Y, Sr, Rb, Th, Pb, Zn, Cu and Ni were also measured in addition to the major elements. The analyzed rocks are dolerite, monzonite, quartz syenite, three representative granites, basalt, trachyte and rhyolite.

The results of the chemical analyses are presented as appendix of this paper. The appendix will be useful to characterize the chemical variation of the Bana complex and be also useful in the further petrological and/or geological studies. Moreover, for the further study of the weathering process of the Bana complex, especially from the stand point of quantitative analyses of chemical weathering, the appendix will be use quite effectively.

In the following section, main chemical characteristics of the constituent minerals and the behavior of trace elements will be described briefly.

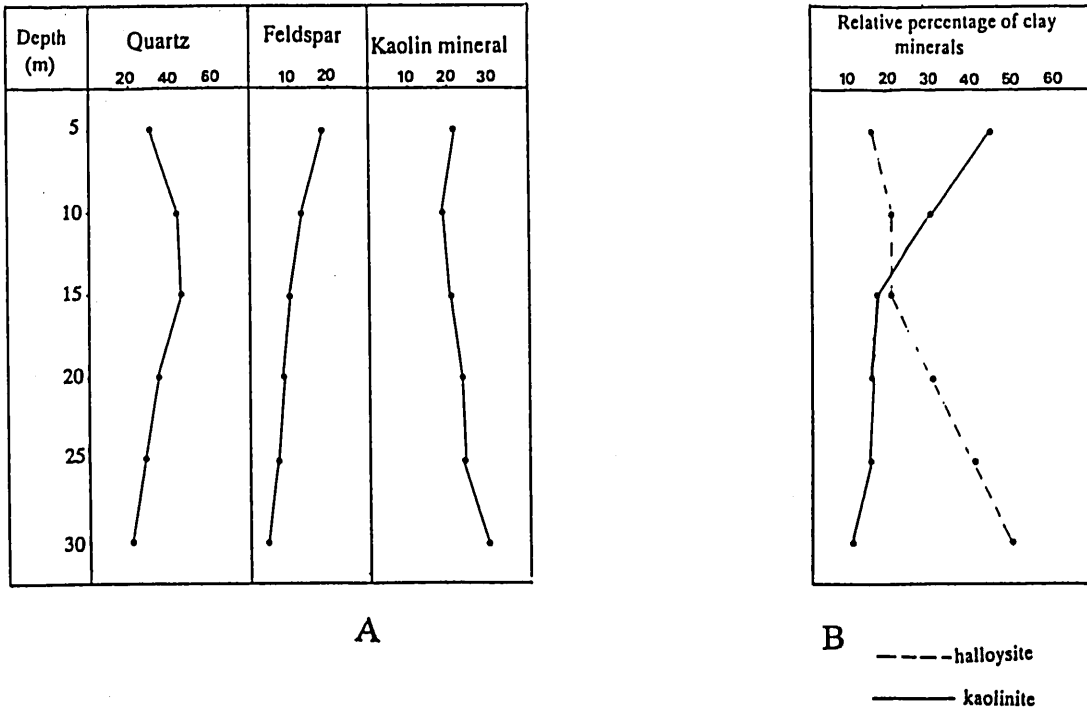


Fig.8 Variation of the constituent minerals of the bulk sample (A) and clay mineral (B) as function of depth on weathered granite.

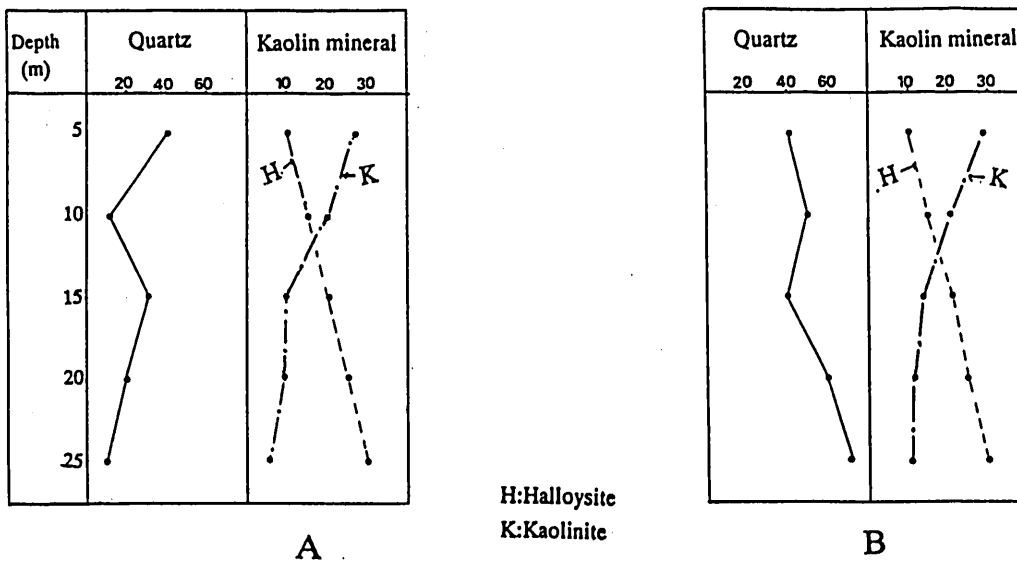


Fig.9 Variation of the constituent minerals as function of depth on weathered basic volcanic rocks (A) and acid volcanic rocks (B).

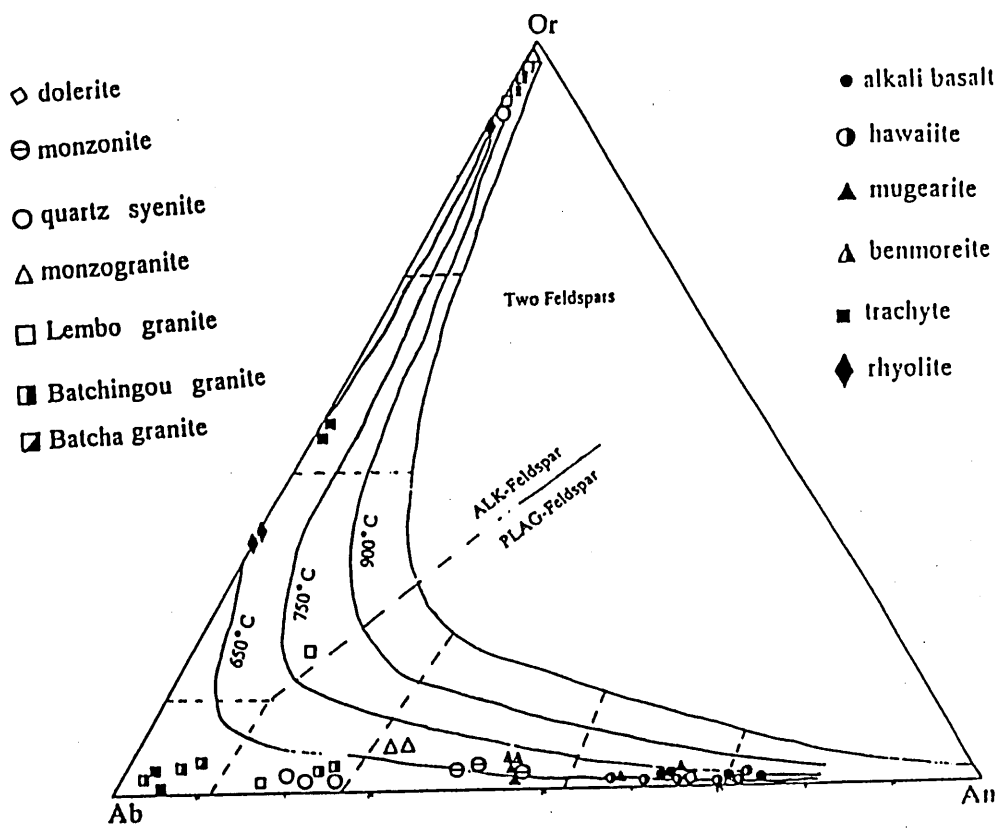


Fig.10 An-Ab-Or ternary diagram with Seck's isotherms of feldspar contained in the Bana complex.

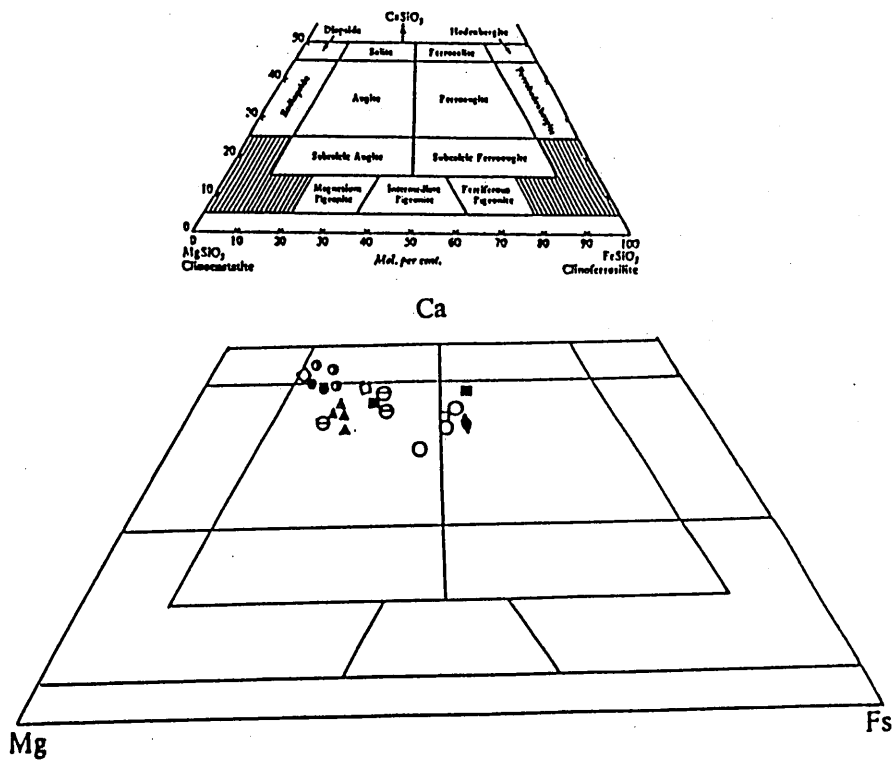


Fig.11 Chemical composition of pyroxenes found in the Bana complex. Classification diagram is taken from that of Poldervaart and Hess (1951).

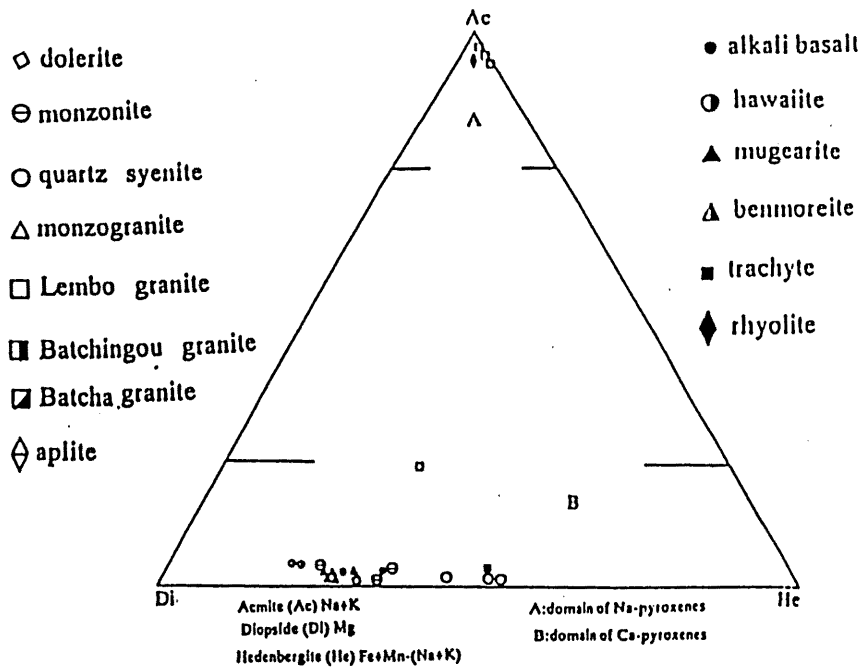


Fig.12 Chemical composition of pyroxene contained in the Bana complex (classification is taken from Aoki, 1964).

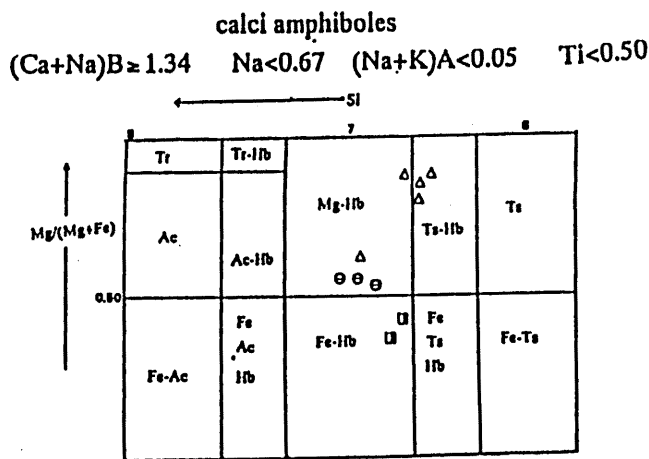


Fig.13 Variation of amphiboles composition in the Bana complex. Classification is that of Leake's (1978).

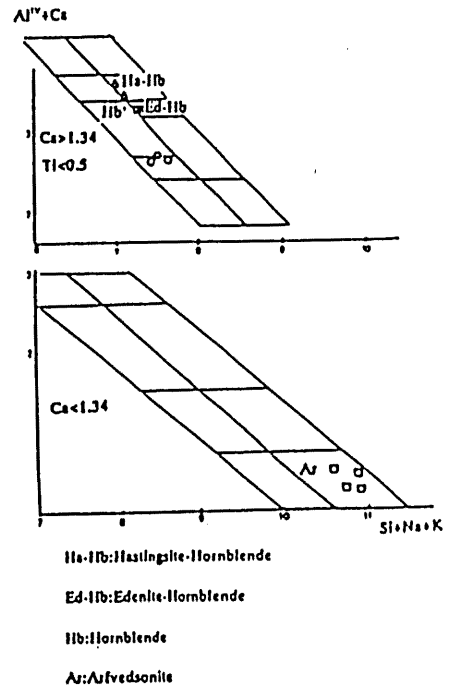


Fig.14 Composition of hornblende represented in Ca+Al versus Si+Na+K diagram.

2A MICROPROBE ANALYSIS

- Feldspar

Plagioclase in dolerite is labrador An66-An60 whereas those in monzodiorite (Nana, 1988) and monzonite are andesine An46-An40. In the quartz syenite, monzogranite and granite, composition of plagioclases vary from andesine An43, oligoclase An15 to albite An6 suggesting a progressive evolution from dolerite An66 to granite An6. In the volcanic rocks, plagioclase in basalt is bytownite An72, labrador An66 and andesine An46 and in trachyte albite An6 indicating progressive evolution from alkali basalt An72 to trachyte An6.

K-feldspar ranges from orthoclase Or92 to Or95 in the intermediate volcanics. In the acidic rocks, composition range is more wide from albite (Ab99) to orthoclase (Or98). In the plutonic rocks of the Lembo, the Batchingou and the Batcha granite composition is richer in potassium (Or98-95). In the volcanic rocks of trachyte and rhyolite K-feldspar is sanidine and anorthoclase to orthoclase respectively (Fig. 10).

- Pyroxenes

Detailed chemical compositions of pyroxene are given in Appendix in which structural formulae are calculated on the basis of 6 oxygens and the splitting of iron into Fe^{3+} and Fe^{2+} is done fixing the total number of cation to 4. According to the nomenclature proposed by Poldervaart and Hess (1951) in the system $Ca/Mg/Fe^{3+}Fe^{2+}Mn$ (Fig. 11). Ca-pyroxenes in the Bana complex vary from diopside, salite-augite to ferro-augite. Clinopyroxenes in basic rocks (dolerite) lie close to the boundaries of diopside-salite and salite-augite whereas those in the intermediate plutonics are augite and ferro-augite. Among the acid rocks only the Lembo granite contains clinopyroxenes of ferro-augite and aegirine. Volcanic rocks in the Bana complex salite and augite are contained in basic lavas and augite and ferro-augite in trachyte. On the actmite-diopside-hedenbergite diagram of Aoki (1964) (Fig. 12) the compositional evolutionary trend can be seen from the calcic to soda rich clinopyroxenes. In the domain of Na-rich pyroxene (A in Fig. 12) aegirine having the highest proportion of actmite occurs in the Lembo granite and rhyolite. In the domain of calcic clinopyroxenes (B in Fig. 12) augite and ferro-augite are found in the basic and intermediate volcanics. Between the two domains, immiscibility or compositional gap is proposed by Aoki (1964). Pyroxenes in the basic rocks have high amount of Ca and Mg while those in the acid rocks small. All the examined pyroxenes contain no Cr and Mn content is small less than 1%.

- Amphiboles

Chemical compositions of amphiboles are given in Appendix in which structural formulae have been calculated on the basis of 23 oxygens. Separation of iron into Fe^{3+} and Fe^{2+} was done with a computer program using the method of Laird and Albee (1981) and names are followed to that proposed by Leake (1978) (Fig. 13). The Bana complex contains two types of amphiboles. 1) Calcic amphiboles: cummingtonite, magnesio-hornblende, magnesio-hastingsitic hornblende, ferro-edenitic hornblende, ferro-hornblende, tchermakitic-hornblende.

2) Sodic amphiboles:arfvedsonite and magnesio-arfvedsonite.

Calcic amphiboles are magnesio hastingsite and magnesio hornblende found mainly in basic rocks (dolerite). The same amphiboles are present in monzonite where they are associated with pyroxene. In monzonite one crystal of cummingtonite has been identified suggesting the result of crustal contamination. In the monzonite magnesio-hornblende and magnesio-hastingsitic hornblende are also found. In quartz syenite, calcic amphiboles are less frequent. In the Batchingou granite, calcic amphiboles are ferro-edenitic hornblende with moderately pleochroic nature.

Sodic amphiboles are found only in the Lembo granite in which ferromagnesian minerals such as magnesio arfvedsonite are predominant.

In the $Ca+Al^4$ versus $Si+Na+K$ diagram (Giret *et al.*, 1980) (Fig. 14) two compositional trends are recognized, one with high values of $Ca+Al^4$ (between 2.6-3.4) and $Si+Na+K$ (between 7.2-7.8) the other has low value of $Ca+Al^4$ (less than 0.5) and highest $Si+Na+K$ (between 10.8-11.2).

- Olivines

Olivine in alkali basalt is fosterite 83% Fo, 85% Fo in hawaiiite, 71% Fo in benmoreite. The evolution of olivine with the differentiation is characterized by the decreasing in fosterite ratio. The manganese ratio seems to be the same in ankaramitic basalt (0.2-0.6%) closed to basanite of Roumpi (Nkombo, 1990) and Nganha (Nono, 1987) resulting a negative correlation against fosterite content (Fig. 15). Ca content in olivine in lava is in the range of 0.6-0.7 (Fig. 16) showing also negative correlation against fosterite content.

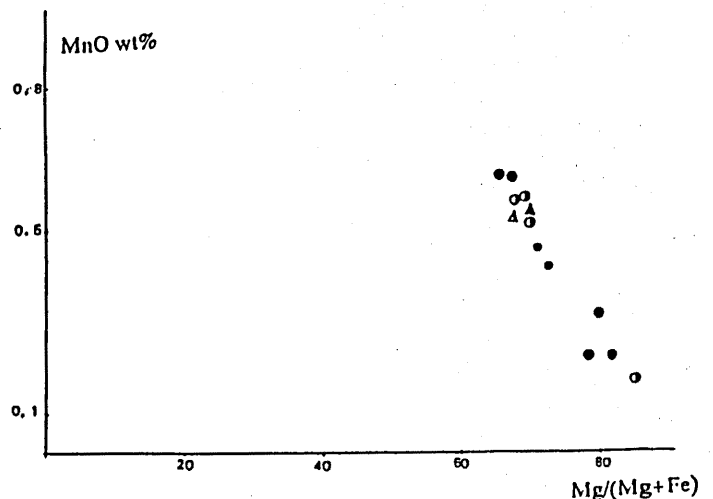


Fig.15 Variation of Mn content in olivine (in lavas of the Bana complex).

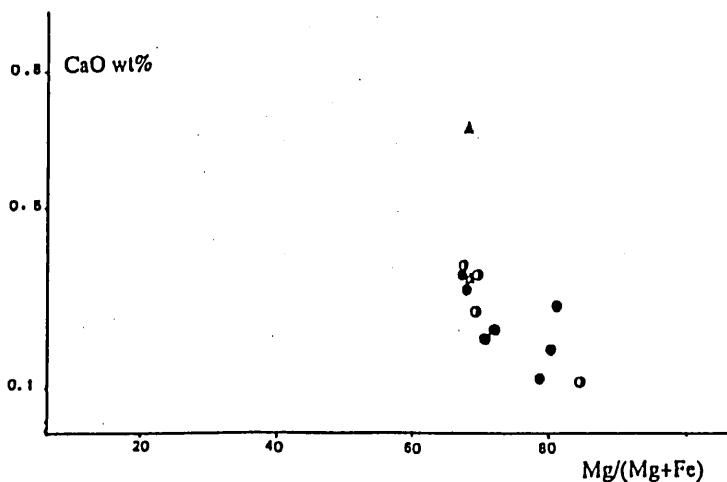


Fig.16 Variation of Ca content in olivine (in lavas of the Bana complex).

2B X-RAY FLUORESCENT ANALYSIS

Representative samples of the various host rock were analysed for major and trace elements by XRF. The main purpose of the analyses are to confirm variation tendency in the chemical composition with increasing weathering. To characterize chemical composition, silica contents were used as differentiation index (Harker, 1909). Fig. 17 shows the variation of major elements in the plutonic rocks as a function of silica content. The results of major elements analyses in plutonic rocks are given in Appendix B-1.

SiO₂ content increases from 50% in dolerite to 72% in biotite granite whereas that in intermediate plutonic is 57-62%.

Al₂O₃ shows a positive correlation against silica from basic rocks (11%) to granite (16.4%). Normative corundum increases from monzonite to granite.

Fe₂O₃ content decreases from 8.86% in basic rocks to 1% in granitic rocks whereas that in intermediate decrease from 8% in dolerite to 3-2% in monzogranite. Normative hematite decreases in the same order.

MgO shows the same variation as Fe₂O₃ being more enriched in the less differentiated types varying from 3.9% in dolerite to 0% in granites. In all the types of the Bana complex MgO/Fe₂O₃ is less than unity.

CaO content shows a negative correlation from the basic rocks (dolerite 8.66%) to acid rocks (0.5-1%). Normative anorthite varies from 24% in dolerite 11-7% in intermediate plutonic and to 6-0% in granite.

Na₂O content varies from 2-3% in basic rocks, 3-4% in intermediate rocks to 4-5.5% in acid rocks. The value of 4-5% in acid rocks (granite) confirms the content of Na-amphibole and Na-pyroxene. Normative albite varies from 27.75% in dolerite to 47% in granite.

K₂O content shows a positive correlation from basic rocks to acid rocks, i.e., from 2.34% in dolerite to 5.84% in granite. Normative orthoclase increases in the same order.

TiO₂ content is very low in basic rocks (dolerite) and in all samples less than 2%. Normative ilmenite and rutile decreases from 4.45% in dolerite to 0.2% in granite.

The results of major elements analyses in volcanic rocks are given in Appendix B-3.

SiO₂ content increases from 45% in basalt to 73% in rhyolite. In basaltic rocks, silica content varies such as

hawaiite (49-50%), mugearite (50-55%) and benmoreite (55-59%). In trachyte silica varies from 62 to 65%. In most weathered rocks silica content is small compared with that of the host rocks.

Al₂O₃ content decreases steadily from basalt (16.87%) to rhyolite (9.81%). Two groups are recognized in rhyolite: one with low amount 9-11% and the other with high (Fig. 19). This high amount of alumina can be explained by the weathering of rocks and formation of normative corundum from 0.4 to 3.56.

Fe₂O₃ content varies from 9% in basic rocks (basalt) to 1.5% in acid rocks (rhyolite). Normative hematite decreases in the same order. Similar to the case of Al₂O₃ content two groups in rhyolite can be distinguished: one with great amount of Fe₂O₃ (6-7%) and another with small amount (1.5-2%).

MgO content decreases clearly from basic rocks (basalt 8%) to acid rocks (rhyolite 0%). In the both types, MgO/Fe₂O₃ is less than the unity.

CaO content shows the same variation like that of MgO. The content varies from 10% in basalt to less than 1% in rhyolite. Normative anorthite decreases from 33% in basalt to 1-0% in rhyolite.

Na₂O shows a steady increasing from basic rocks (2.6% in basalt) to acidic rocks (4.8% in rhyolite). Normative albite increases from 14% in basalt to 60% in rhyolite.

K₂O shows a positive correlation from basic rocks (0.5% in basalt) to acid rocks (6% in rhyolite) like Na₂O. Normative orthoclase varies in the same order, from 3.5% in basalt to 36% in rhyolite.

TiO₂ content decreases from basic rocks to acid rocks. It varies from 3% in basalt to 0.3% in rhyolite. The values correspond to normative ilmenite from 3% in basalt to 0.1% in rhyolite.

Sr is 512ppm in dolerite and increases towards the intermediate rocks from 403ppm to 912ppm. The content in quartz syenite is 368ppm, 115 to 54ppm in Batchingou granite, 162 to 10ppm in Lembo granite and 42 to 36ppm in Batcha granite. These characteristics are presented in Fig. 19. The value is 859ppm in alkali basalt, decreases from 1091ppm to 181ppm in intermediate volcanics. However, abnormally high values are observed in hawaiite (1091ppm) and mugearite (1063ppm) compared with low content of 352-181ppm in trachyte and 20ppm to less than 10ppm in acid rock (rhyolite) (Fig. 20).

Sr/SiO₂ diagram (Fig. 19d) shows a negative correlation from dolerite to granite. The intermediate rocks shows a slight positive correlation. In the volcanic series negative correlation from basalt to rhyolite is recognized (Fig. 20n). According to the previous results such as Heir and Adam (1964), Sr can replace K position more readily than Ca position because Sr/Ca ionic ratio is about 10 times. This can reasonably explain the present result.

Rb content varies from 53ppm in dolerite to 218ppm in granite whereas in volcanic rocks the content varies from less than 10ppm in basalt to 166ppm in rhyolite (Figs. 19e and 20o). In the Rb/SiO₂ diagram (Fig. 19e) positive correlations from basic rocks to intermediate rocks and from syenite to granite are recognizable. Since biotite and orthoclase can contain more Rb increasing of

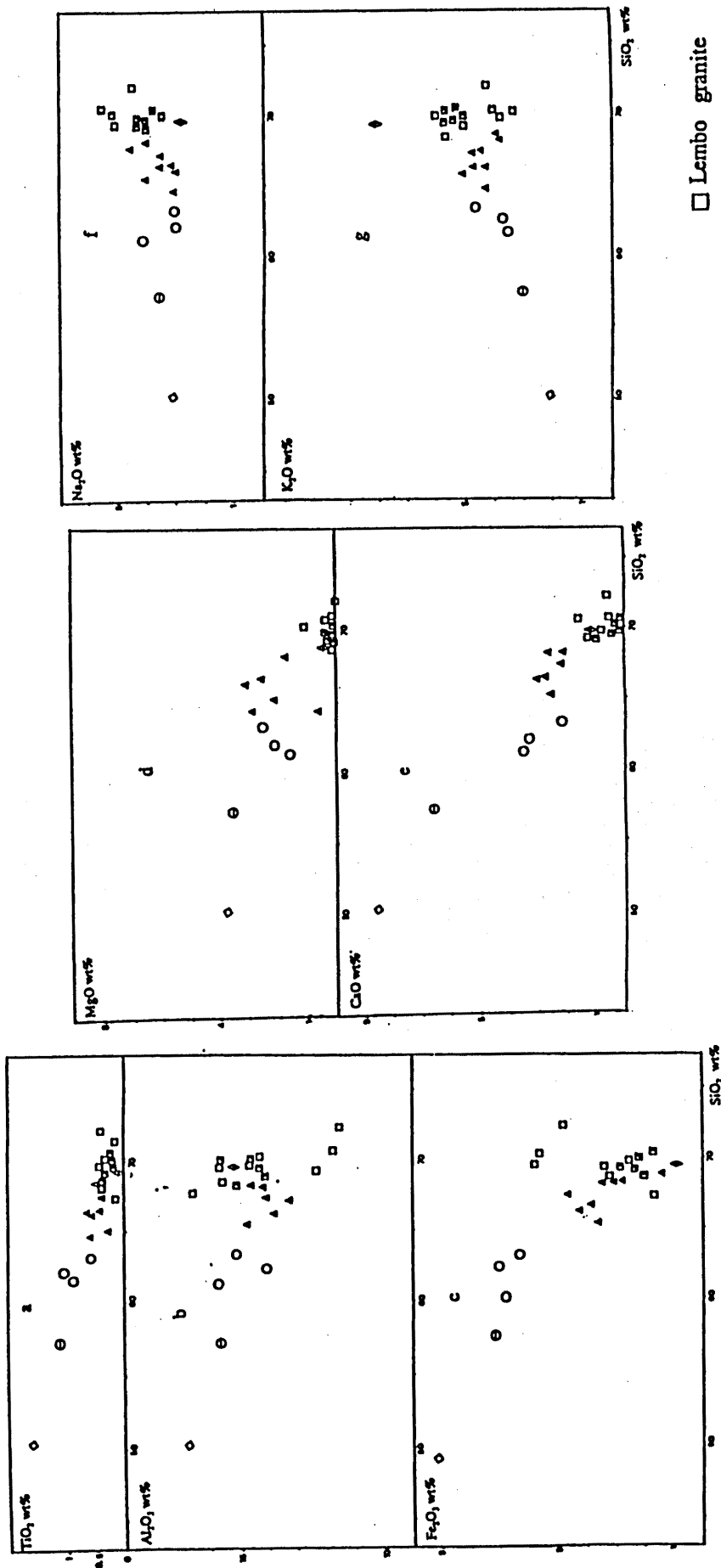


Fig.17 Variation tendency of major elements in the plutonic rocks found in the Bana complex as a function of silica content.

- ◇ dolerite
- monzonite
- quartz syenite
- △ monzogranite

- Lembo granite
- Batchingou granite
- ▨ Batcha granite
- ◇ aplite

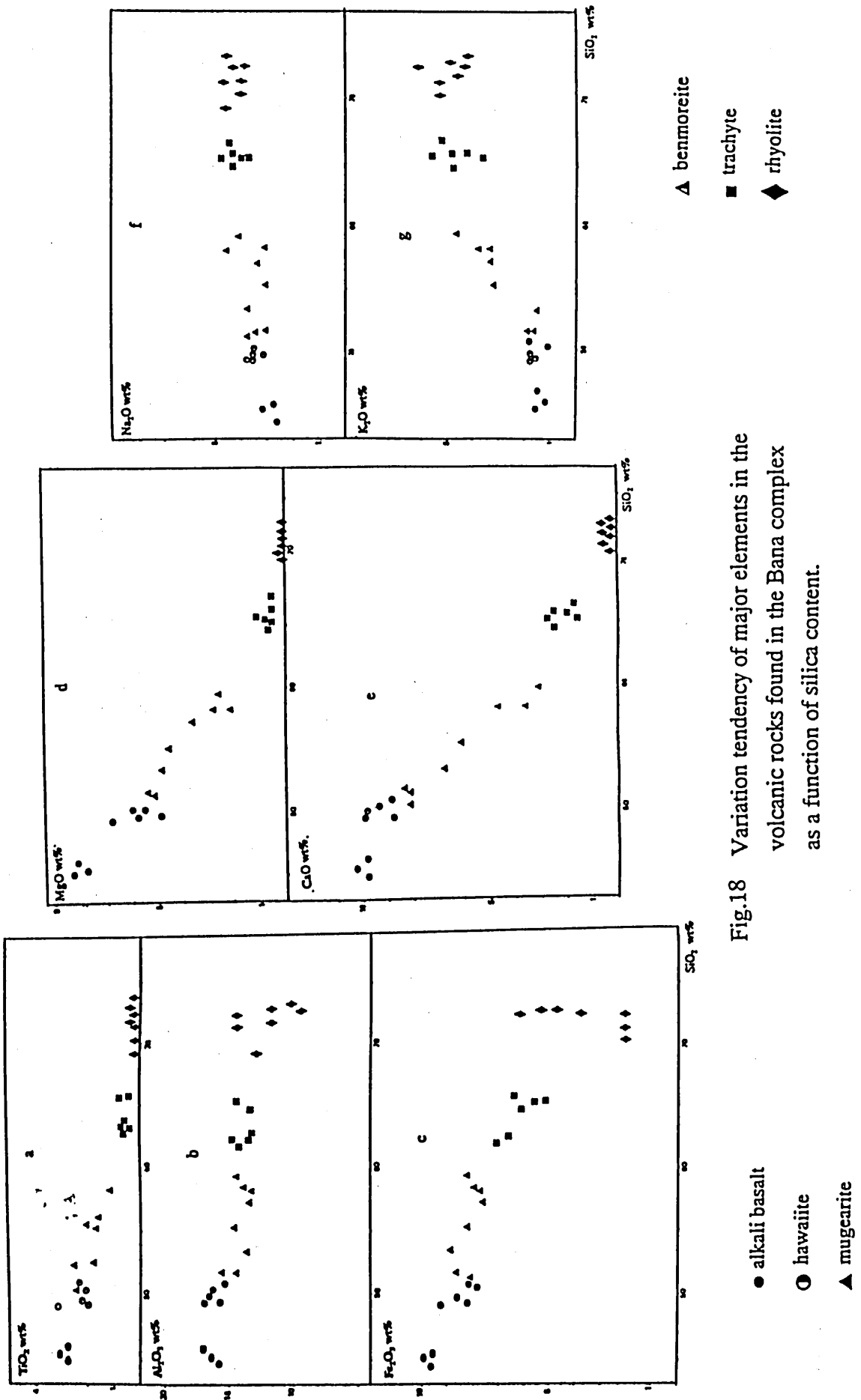


Fig.18 Variation tendency of major elements in the volcanic rocks found in the Bana complex as a function of silica content.

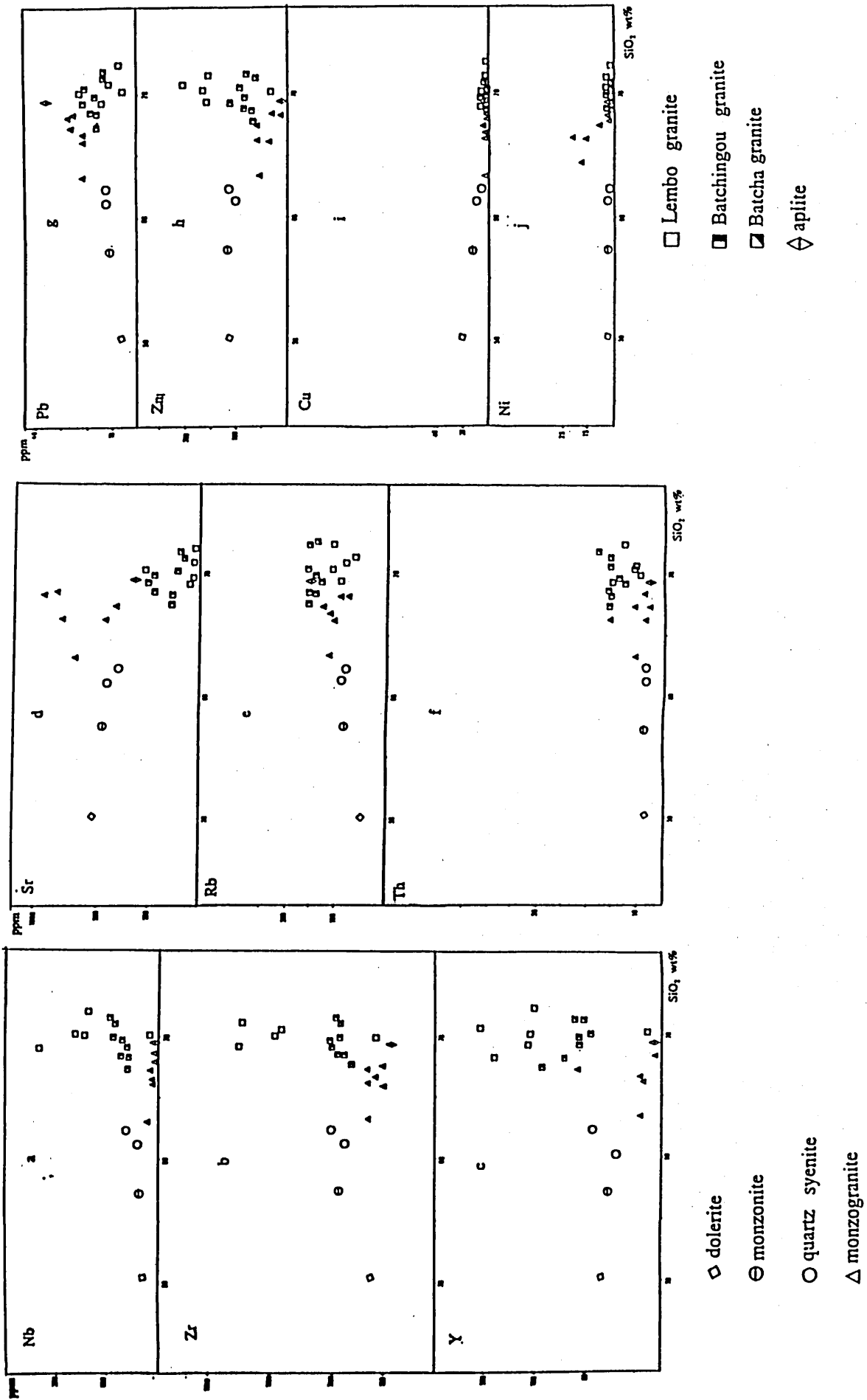


Fig.19 Variation of trace elements contained in plutonic rocks (a---j) of the Bana complex.

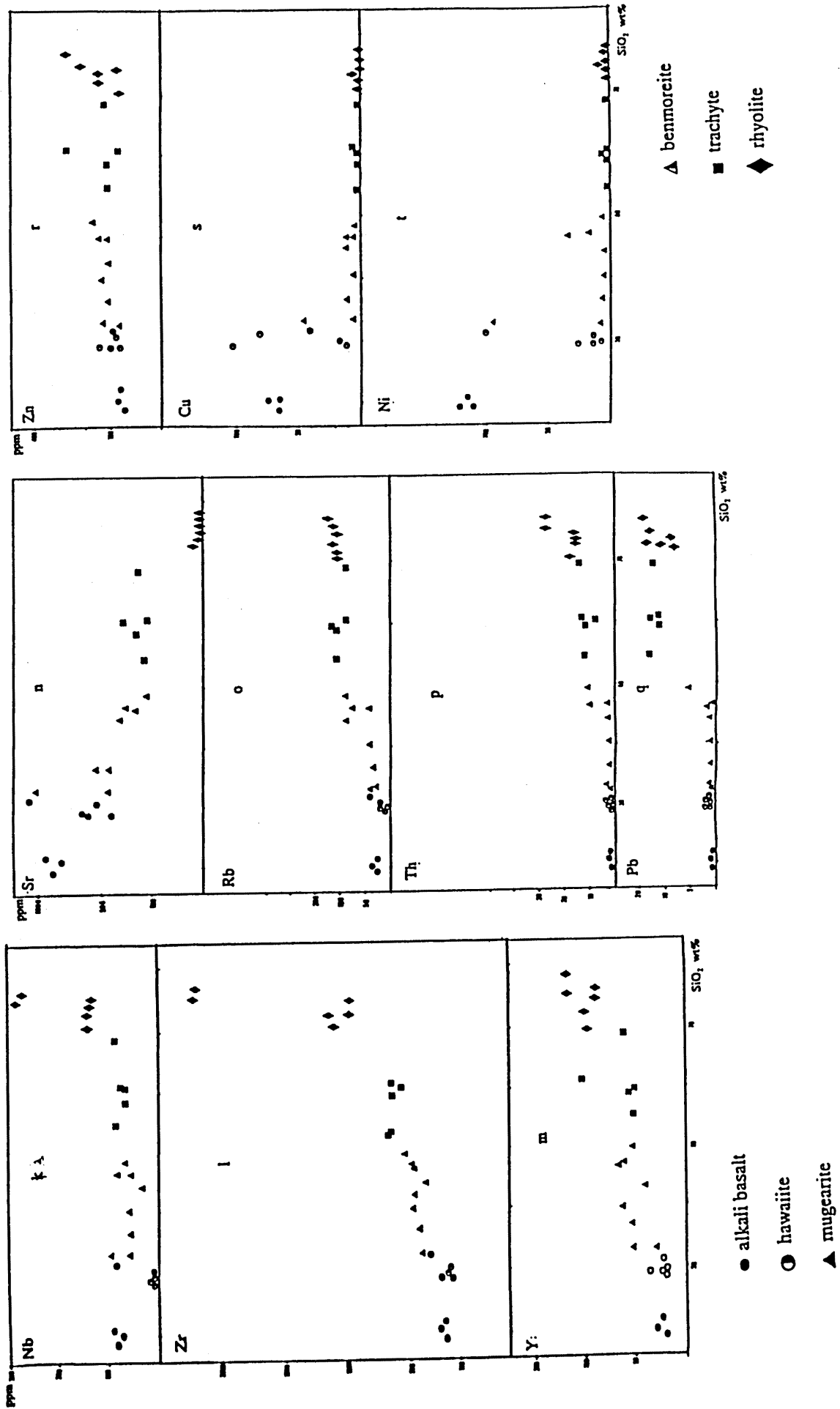
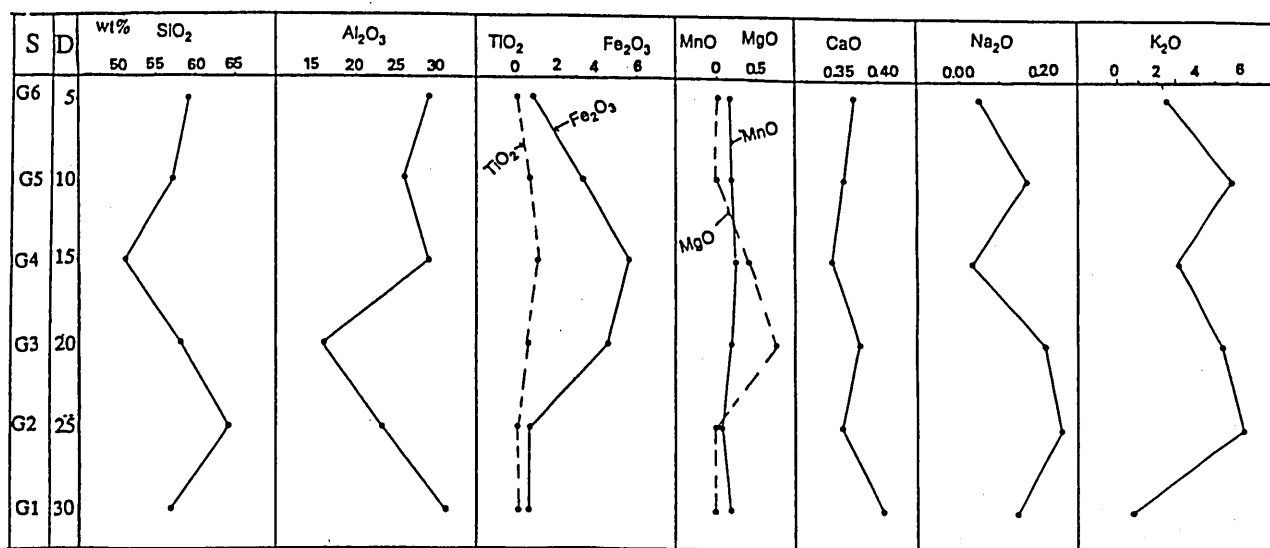
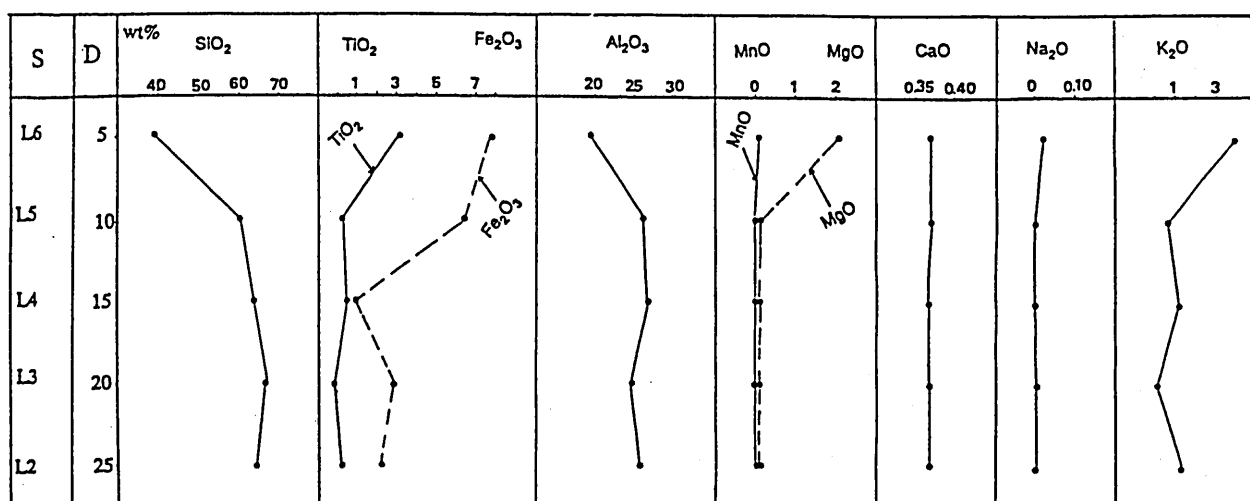


Fig.20 Variation of trace elements contained in volcanic rocks (k---t) of rocks of the Bana complex.



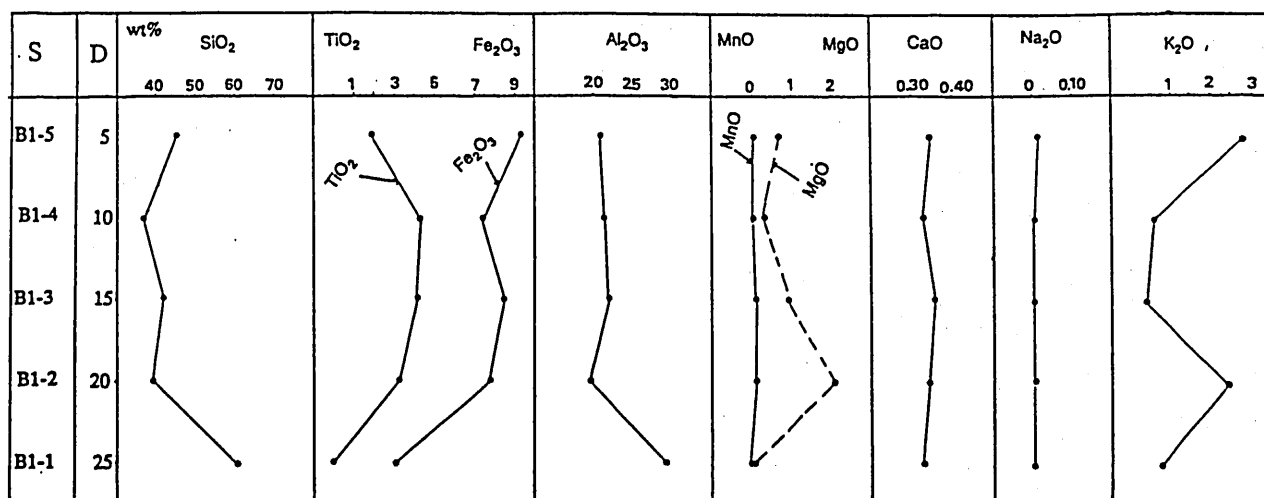
S:sample
D:depth (m)

Fig.21 Variation of major elements with depth in weathered Lembo granite.



S:sample
D:depth (m)

Fig.22 Variation of major elements with depth in weathered acid volcanic rocks.



S:sample
D:depth (m)

Fig.23 Variation of major elements with depth in weathered basic volcanic rocks.

fractionation is responsible for positive correlation.

Th content varies from 10ppm in basic and intermediate rocks to 17ppm in acidic rock (Batchingou granite). In volcanic suite it varies from less than 10ppm in basic rocks to 28ppm in acidic rock (rhyolite) (Figs. 19f and 20p).

Zr content varies from 246ppm in basic rocks to 1266ppm in acidic rocks (Lembo granite) in the plutonic series. In the volcanic series Zr content varies from 176ppm in basic rocks to 2236ppm in acidic rock (rhyolite) (Figs. 19b and 20l).

Y content varies from 46ppm in basic rocks to 149ppm in acidic rocks in the plutonic series. In the volcanic series Y content varies from 24ppm in basic rocks to 232ppm in acidic rock (Figs. 19c and 20m).

Ni content is less than 10ppm in all plutonic rocks. In volcanic rocks the content varies from 191ppm in basic rocks to less than 10ppm in acidic rock (Figs. 19g and 20t).

Cu content varies from 22ppm in basic rocks to less than 10ppm in acidic rocks in plutonic series. In volcanic series, the value varies from 117ppm in basic rocks to less than 10ppm in acidic rock (Figs. 19i and 20s).

Zn content is 135ppm in basic rocks, decreases in intermediate rocks 35ppm and increases in acidic rocks 342ppm (Lembo granite). In volcanic suite the content varies from 8ppm in basic rocks to 290ppm in acidic rocks (rhyolite). Nb content varies from 34ppm in basic rocks to 231ppm in acidic rocks (Lembo granite), whereas in volcanic suite it varies from 24ppm in basic rocks to 296ppm in acidic rock (rhyolite) (Figs. 19a and 20k).

Chemical composition of weathered samples given in Appendix B-5, B-6 and B-7 shows rather complicated variation and the fact reflects probably the degree of alteration of mainly weathering. In bulk samples collected from granite loss of SiO_2 , CaO and Na_2O is generally recognized whereas Al_2O_3 and TiO_2 contents remain almost constant. As seen in Fig. 21 SiO_2 and Al_2O_3 contents vary rather complicatedly with depth. This variation can be ascribed to the change such as pH and temperature during weathering. To be noted is that the variation of silica and alumina contents can be correlated to formation of kaolin minerals such as halloysite and kaolinite. That is XRD pattern shows halloysite is rich in the lower part, halloysite and kaolinite in the middle part and kaolinite is rich in the upper part. Variation of Fe_2O_3 content can be correlated to the presence of hematite or goethite of which the existence of the later mineral was confirmed by XRD. CaO content is constant along the profile. Na_2O and K_2O show the same correlation. Content of Na_2O remains very low compared with the host rock indicating its rapid loss.

In the bulk samples collected in acidic volcanics slight loss of SiO_2 and Fe_2O_3 and rapid loss of CaO, Na_2O , K_2O are confirmable. As seen in Fig. 22, SiO_2 content tends to increase with increasing depth. The small amount of SiO_2 (39.79wt%) in the upper part of profile indicates the active leaching and the fact well corresponds to the small amount of kaolinite. TiO_2 and Fe_2O_3 tend to decrease with increasing depth. The great amount of Fe_2O_3 (7.94wt%) in the upper part suggests formation of goethite or hematite and the fact is well confirmed by XRD

results. Al_2O_3 content tends to increase with increasing depth. Na_2O leaches completely from the host rocks and the same tendency is recognized in the behavior of K_2O .

In the basic rocks a slight loss of SiO_2 , rapid loss of MgO , CaO, Na_2O and K_2O are remarkable. TiO_2 and Fe_2O_3 remain constant whereas Al_2O_3 content increases. As seen in Fig. 23 SiO_2 tends to increase with increasing depth. High content (60.58wt%) of silica in the lower part indicates precipitation to form halloysite. Fe_2O_3 tends to decrease with increasing depth but it remains high in all portion of the profile. Al_2O_3 content increases with increasing depth. CaO content is low and is constant along the profile.

Chemical composition of weathered rocks of various types in the Bana complex represented in the CaO- Na_2O - K_2O diagram (Fig. 24) shows clear decrease in potassium, sodium and calcium content.

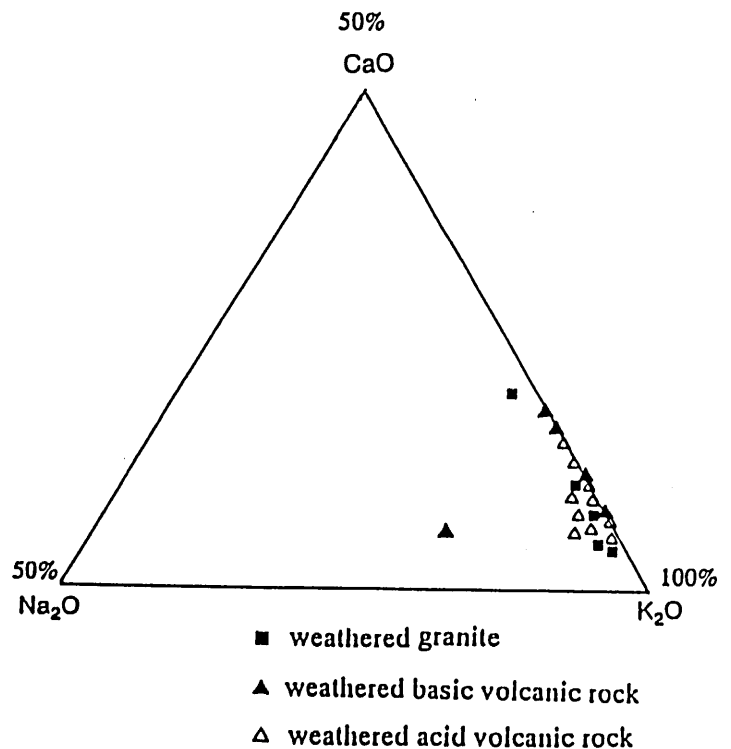
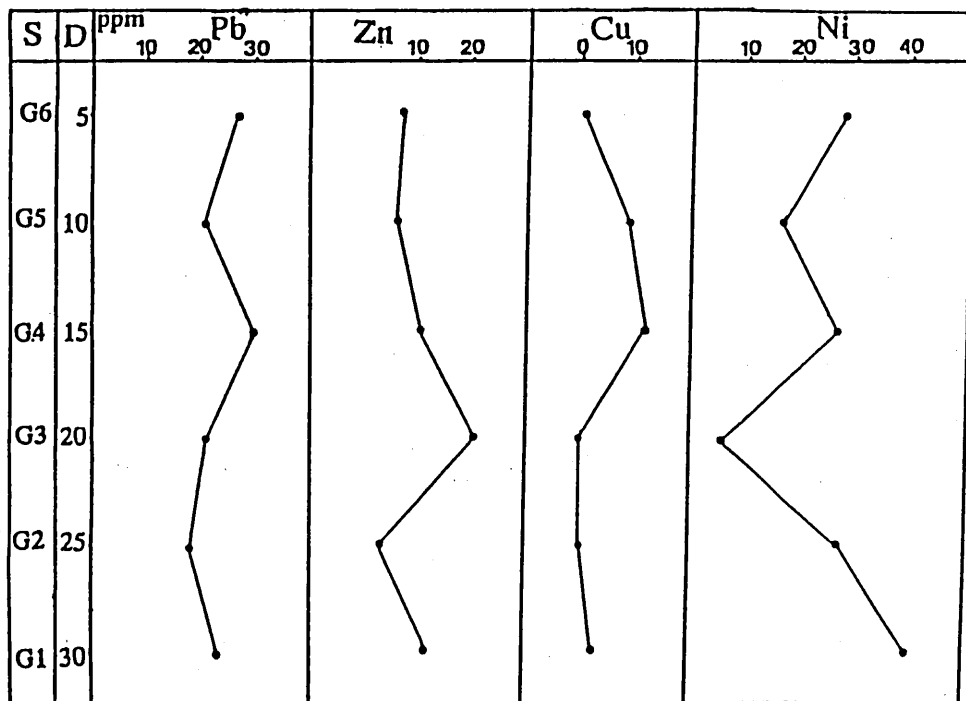
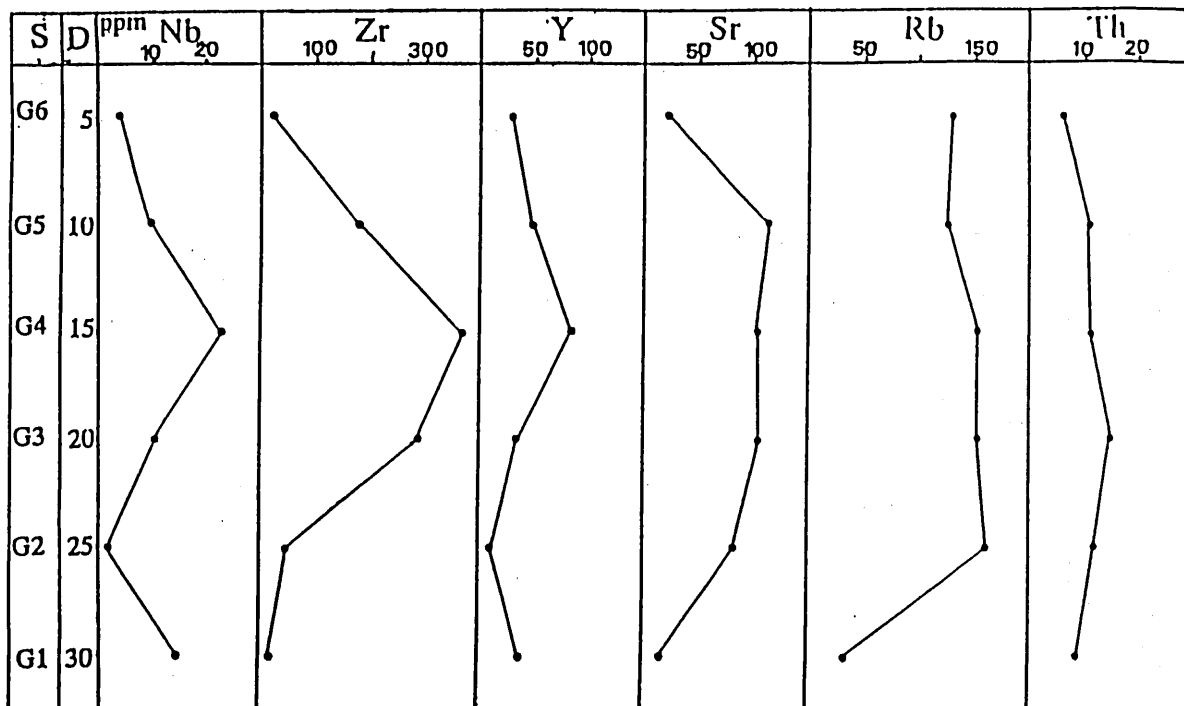


Fig.24 CaO- Na_2O - K_2O diagram of major elements contained in weathered Lembo granite and weathered volcanic rocks.

Results of trace elements analyses are presented in Appendix B-5, B-6 and B-7. Nb content is lower in weathered granite and weathered volcanic rocks compared with that of respective host rocks. Zr content is high in volcanic rocks (acidic:1301-1672ppm; basic:147-748ppm) compared with that of granite (20-373ppm). Y content is high in acidic volcanics (153-465ppm) compared with that of plutonic rocks (9-87ppm). Sr content shows no characteristic features against the rock types. Rb content in acidic volcanics is relatively low. Th, Pb and Zn are almost constant through all the rock types. Cu content is less than 10ppm in all rocks types. Ni content in granite (48-140ppm) is relatively high.

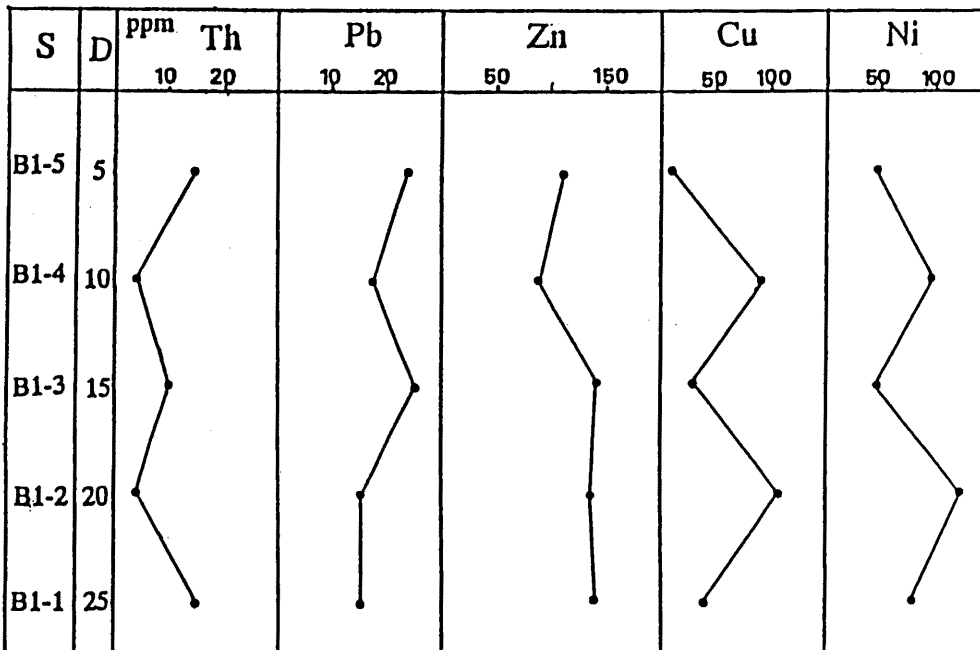
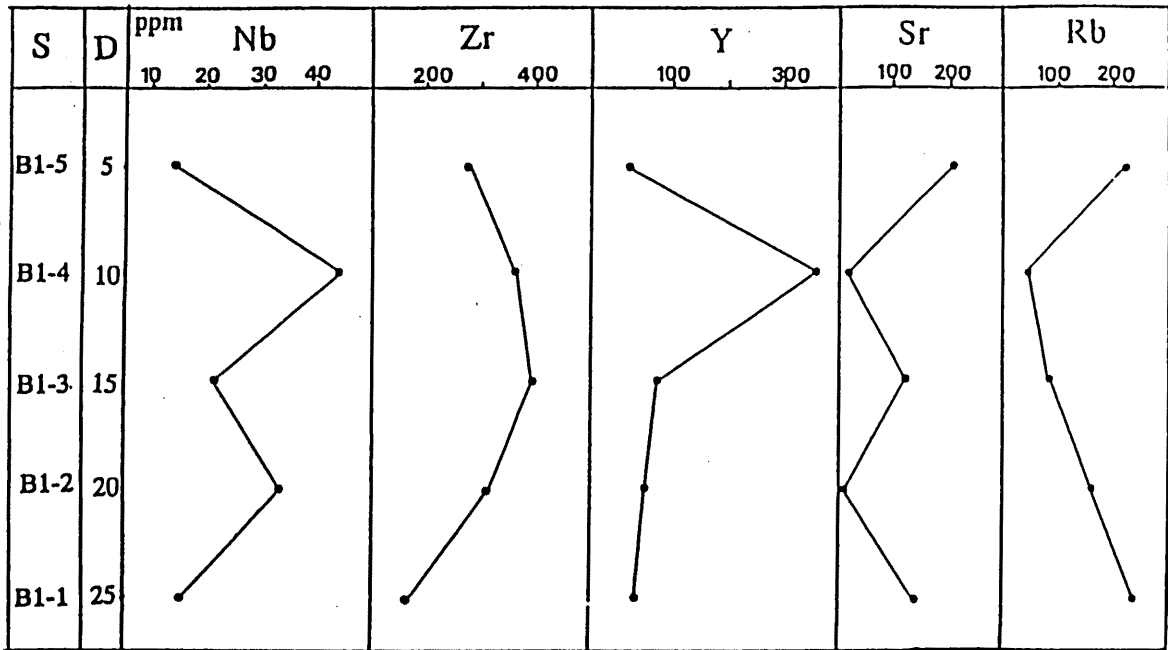
Examination of trace elements revealed that:1) rapid loss of Nb and Zr in weathered Lembo granite, 2) a slight loss of the same elements in the acidic volcanics, 3) Y is



S:sample

D:depth (m)

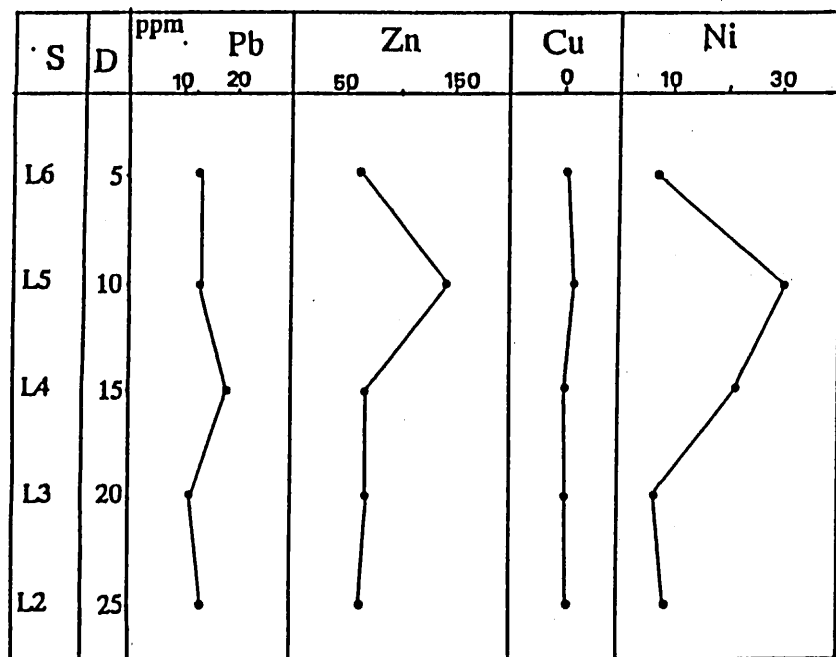
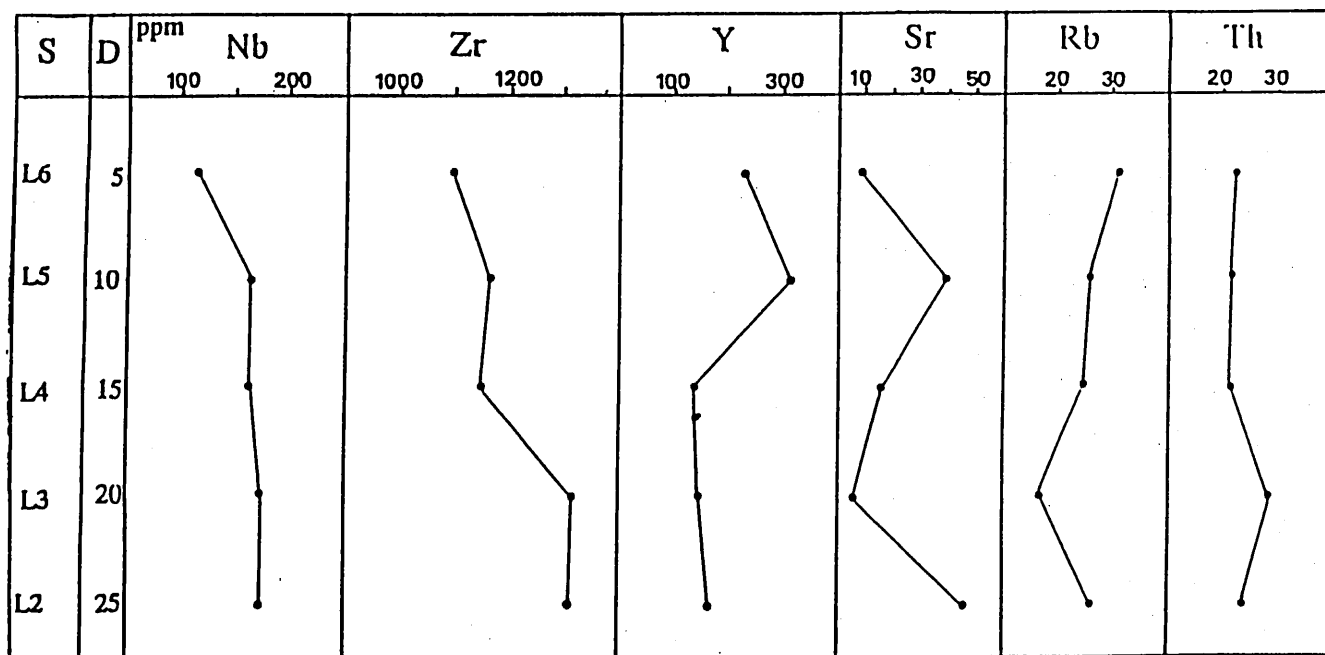
Fig.25 Variation of trace elements with depth in weathered Lembo granite .



S:sample

D:depth (m)

Fig.26 Variation of trace elements with depth in weathered basic volcanic rocks.



S:sample
D:depth (m)

Fig.27 Variation of trace elements with depth in weathered acid volcanic rocks.

gained in weathered acidic volcanics, 4) Sr content decreases rapidly in basic and acidic volcanics whereas Rb content decreases considerably in acidic volcanics. Variation of trace elements content in the Lembo granite as function of depth is summarized in Fig. 25. No characteristic tendency from the upper to the lower part can be recognized. Abnormal increase of Nb and Zr content in the middle part should be pointed out. In Figs. 26 and 27, the same examinations on the basic and acid volcanic rocks are presented, respectively. From the lower part to the upper part, Nb, Zr and Sr contents tend to decrease suggesting the effect of weathering.

In conclusion SiO_2 shows a rapid loss in the Lembo granite, a slight loss in acidic and basic volcanic rocks during the weathering process. Fe_2O_3 content remains almost constant in basic volcanic rocks. MgO, CaO, Na_2O and K_2O contents decrease more or less throughout all the rock types as weathering proceeds. Results of chemical analyses of major and trace elements show that most of the major elements decrease through the weathering process and the loss is compensated by addition of water content. This fact can be partly explained by production or formation of hydrous minerals, i.e. clay minerals.

3 SCANNING ELECTRON MICROSCOPE (SEM) OBSERVATION

It has been generally accepted that, halloysite transforms to kaolinite under tropical weathering conditions as was described in the previous. The widespread recent availability of SEM has promoted the morphological examination of minerals, especially that of clay minerals (e.g. quartz, Krinsley and Cavallero, 1970; Schneider, 1970; Krinsley and Doorkamp, 1973; kaolinite, Keller, 1976 & 1977; Kitagawa *et al.*, 1994). Examination of dissolved patterns found on crystal surfaces of remained minerals such as quartz and K-feldspar has recently developed and the results provide significance progress in obtaining information concerning weathering process especially micro-environmental conditions (cf. Kitagawa *et al.*, 1994). Although quartz is one of the most resistant minerals against chemical attack, significant effects of weathering or hydrothermal alteration were recorded on its surface as etch pits. Therefore, morphological variation of the etch pits recorded on the surface of quartz and K-feldspar collected from the bottom to the top of weathered profiles in the Lembo granite and acidic volcanic rocks were examined in this research.

Quartz and K-feldspar were collected from the weathered part of the granite and acid volcanic rocks and their surface was observed by SEM. Numerous etch pits were found. Morphology of etch pits are various such as circular, triangular, hexagonal and irregular shape and the depth of the pits is also various. Etch pits found in the lower and middle part are in general shallow and small whereas those found in the upper part are deep and wide (Plate 1). Quartz grains found in the lower part have generally smooth surfaces whereas those in the middle and the upper part have rough surface with sharp edges. Some K-feldspar grains reveal that the dissolution occurs at certain special part of the crystal surface. Etch pits are in general rectangular, and conical hollows are developed on its surface (Plates 2 and 3). Etch pits observed in the

present research are quite resemble to those reported by Wilson (1978) and Kitagawa *et al.*, (1994). In the Lembo granite number of etch pits on quartz and K-feldspar surfaces decreases with depth and etch pits found in the upper part are more rougher than those in the lower part (Plates 1D, 1C, 1B, 1A, respectively) and (Plates 2D, 2C, 2B, 2A, respectively). In addition to the etch pits observation morphological examination of kaolin minerals gives us further information concerning weathering condition. Morphological variation of the kaolin minerals observed in the present research are shown in (Plate 4). As is shown in this plate halloysite shows relatively smooth surface (Plate 4A and 4B) and kaolinite found in extensively weathered part shows "books" morphology (Plates 4C and 4D).

Several types of aggregation particles gathered in different orientations were identified in undisturbed samples. One type is skeletal-matrix having many porosity (Plate 5A). In this texture pattern, coarse particles are seen as floating in the matrix of flaky clays. Porosity is high and most pores have a diameter between 1 and $2\mu\text{m}$. Large pores with size of more are characteristically dominated. High magnification observation reveals that each aggregation is composed of randomly oriented clay particles (Plate 5A). Hexagonal shape clay flakes in the cluster represent morphological characteristics of kaolin minerals (Keller, 1976). The second type is parallel flaky particles gathered densely with each other (Plate 5B) which found often in the clay fraction collected from basic volcanic rocks. The aggregation has poorly defined outer boundary of the individual clay particles. Some packages are so densely gathered together that the individual clay particles can not be discerned. The third type is so-called flocculent texture (Plate 5C). High magnification view shows that the composed clay particles have smooth surface and wavy boundary. All three types aggregation observed in the weathered granite are quite similar to those appeared in weathered basic and acid volcanic rocks. Texture pattern found in the basic to acid rocks are characterized by randomly oriented particle contacts (Plate 5D). Preferred orientation of clay particles found in the present research may be caused by sheare stress as will be discussed later.

Morphological variation of etch pits developed on quartz and K-feldspar surfaces is most probably caused by difference of the nature of the related solution such as pH during the dissolution process.

4 MORPHOLOGY OF CLAY MINERALS

Electron microscopy has been proved to be of great value in the identification of clay minerals in fine-grained clay fractions. For example, by X-ray diffraction, thermo-analysis and infra-red spectroscopy methods distinguishment between poorly ordered halloysite and well ordered halloysite is not possible. Electron microscopy is also of great importance in the study of clay mineral genesis, e.g. at the formation of halloysite from amorphous phase. In this chapter, morphological variation of kaolin minerals observed under the transmission electron microscope (TEM) will be examined. Halloysite, in general, exhibits a various morphologies including tubes, spheres, plates, oblate spheroids, stubbly

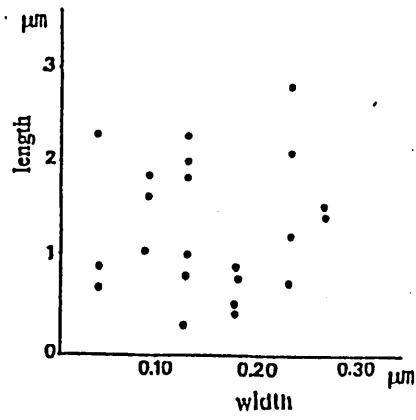


Fig.28 Distribution of length and width of tubular halloysite collected from weathered lembo granite.

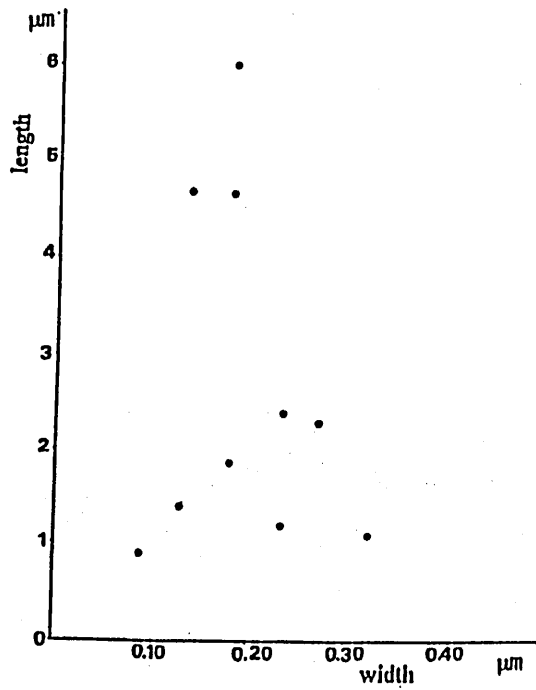


Fig.30 Distribution of length and width of tubular halloysite collected from altered basic volcanic rocks.

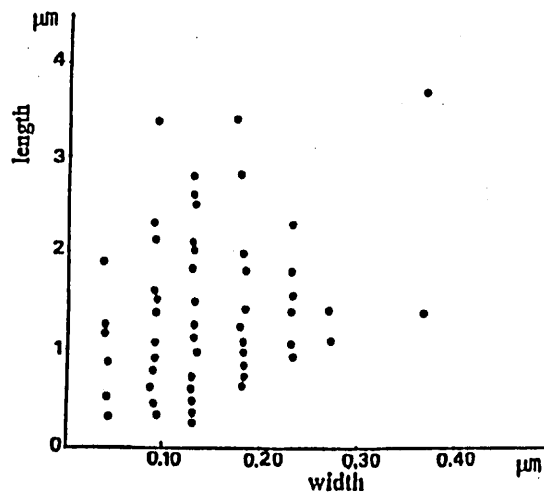


Fig.32 Distribution of length and width of tubular halloysite collected from altered acid volcanic rocks.

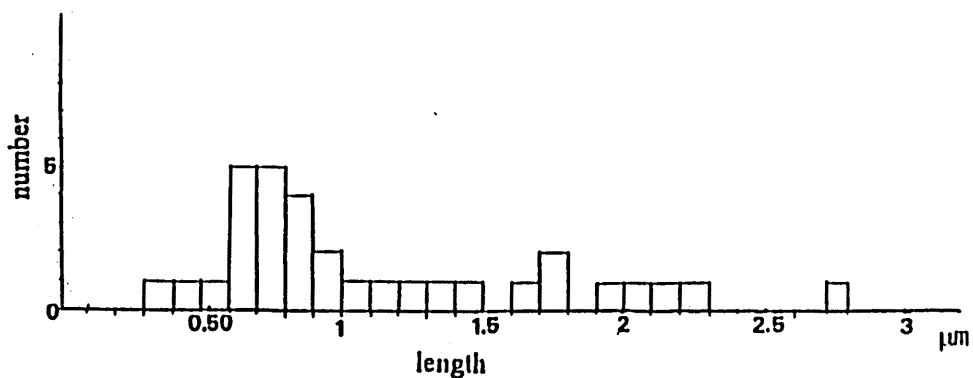


Fig.29 Histogram of length of tubular halloysite collected from weathered Lembo granite.

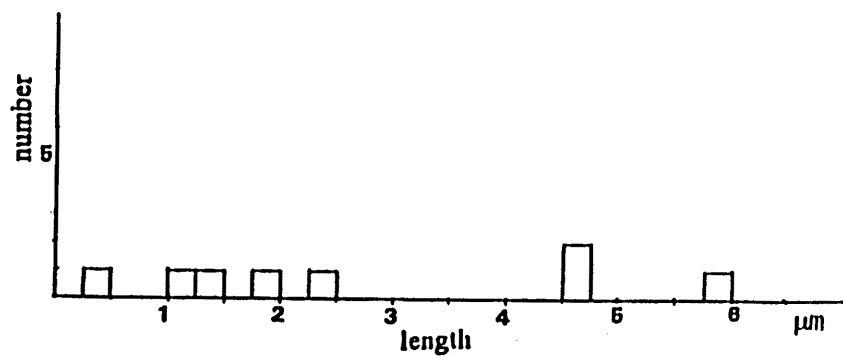


Fig.31 Histogram of length of tubular halloysite collected from altered basic volcanic rocks.

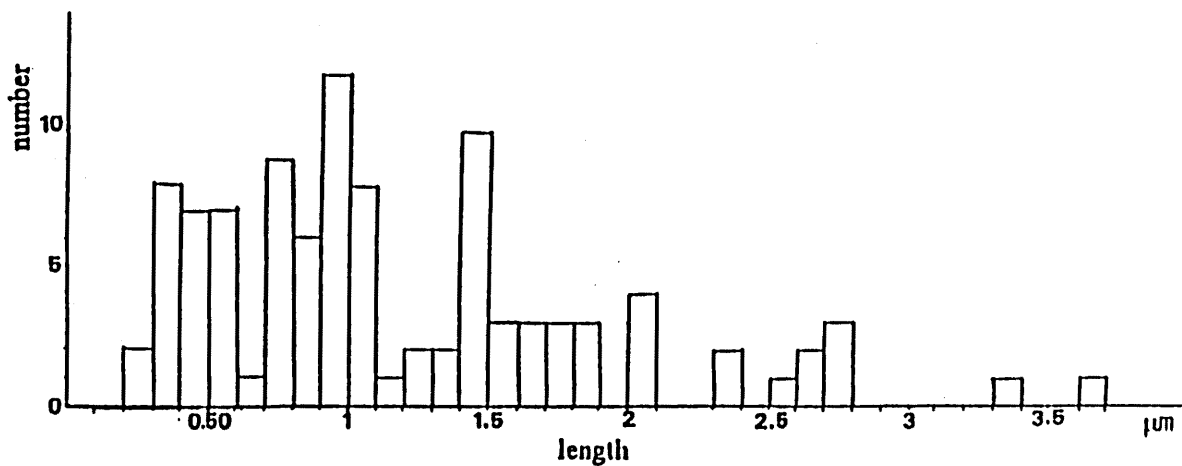


Fig.33 Histogram of length of tubular halloysite collected from altered acid volcanic rocks.

cylinders and irregular shapes (Bates *et al.*, 1950; Dixon and Mc Kee, 1974; Dixon, 1977; Sudo *et al.*, 1980; Kirkman, 1981). Tubular form was once considered as characteristics of halloysite distinguishing from kaolinite (Sudo and Takahashi, 1956; Kurayashi and Tsuchiya, 1960; Okada, 1973; Churchman *et al.*, 1984). Examination of morphology of the clay fractions revealed various morphologies such as spheroid and tubular halloysite, platy kaolinite, needle goethite and amorphous materials.

In weathered Lembo granite the length of halloysite tubes varies from 0.27 to 2.79 μm whereas the width varies from 0.04 to 0.27 μm (Fig. 28). Fig. 29 shows a relation between the length and width of tubular halloysite in which rather high concentration around 0.60-0.90 μm is recognizable. Spheroid halloysite associated with short tubes have average diameter around 0.37-0.55 μm (Plates 6A and 6B).

In weathered basic volcanic rocks halloysite tubes have a maximum length 6 μm (Plate 7B) with various width from 0.09 to 0.32 μm (Fig. 30). No special predominate length (Fig. 31) are recognizable. Goethites are well developed as forms of needle crystals and brush-like bundle. Amorphous materials are also observed (Plate 7C). Spherical halloysites have diameter between 0.23-0.65 μm (Plate 7A).

In weathered acid volcanic rocks, halloysite tubes show wide range of both length and width (Plate 8). The length of the tubes varies from 0.27 to 3.72 μm whereas width varies from 0.04 to 0.37 μm (Fig. 32). Fig. 33 shows frequency of length of halloysite tube. In the range less than 2 μm most of the halloysite crystals are concentrated. Spheroid halloysites are associated with short and long tubes and have diameter between 0.18-0.46 μm (Plate 8A). In conclusion tubular halloysite examined in the present research shows a wide range of length and width. No special relation between the length and width is confirmed. The examined halloysite found in the weathered granites as a whole is characterized by predominance of short tubes and that from weathered volcanic by long tubes. To be noted is that spheroidal halloysite is characteristic in weathered Lembo granite and volcanic rocks in the Bana complex.

Kaolinite is characterized by flaky morphology and the maximum dimension of flake surface is in the range between 0.2 to about 4 μm . Platy flakes are often observed. Edges of the flakes are somewhat ragged and irregular and the hexagonal outline is not common. Such poorly crystallized kaolinite occurs mostly as smaller and thinner particles and commonly found in specimens collected from the upper part of the profiles in granite as well as in volcanic rocks (Plates 6D, 7D and 8D).

V. DISCUSSION

The various igneous rocks composed of the Bana complex are in general extensively weathered under the tropical humid and arid climate. In the preceding, mineralogical characteristics of the host rocks and weathered rocks were examined in detail. Special attentions were paid on the examination of clay fractions such as micro-morphology. Based on the results obtained, alteration condition and/or weathering process will be discussed in the following.

1 Factors controlling weathering process

It is well known that, time is an important factor for alteration process of rock forming minerals especially for slowly proceeding weathering. Although each mineral has its own breakdown rate and the rate varies complicatedly according to weathering condition, mineralogical examinations performed in the present research can not give significant information on the kinetics of weathering. Climate of the district play certain role in accelerate weathering reaction together with topography of the district. In addition to the heavy rainfall of the district (Fig. 34), steep topography and drainage (Figs. 35 and 36) promote leaching the elements contained in the host rocks. The average altitude of the district is about 1500m and the topographical characteristics produce steep slopes in many locations. Weathering crust is thin in such place but thick weathering crusts are developed commonly excepts such special locations. The thick weathering crust is caused mainly by severe climate, i.e., temperature and rainfall as it pointed out by Lasaga *et al.*, (1994).

The average rainfall during past 26 years (Table 1) is about 1700mm in this district. Under such conditions, chemical weathering proceeds rapidly resulting soil rich in clay minerals and alumino-silicates such as gibbsite, kaolinite and halloysite. Moreover, common weathering products of kaolin minerals regardless the kind of the host rock may probably be ascribed to the severe natural environmental conditions of the district.

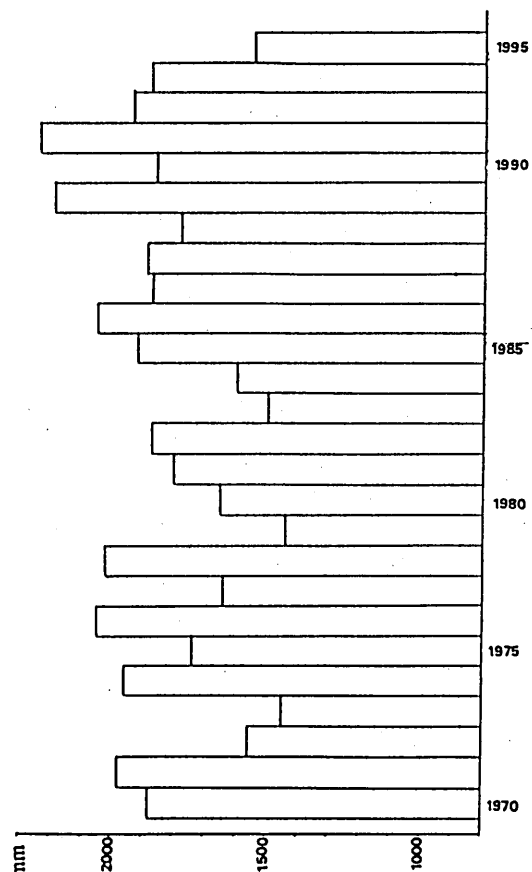


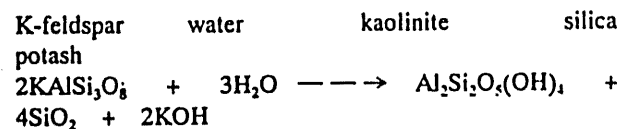
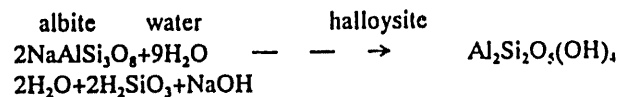
Fig.34 Histogram of rainfall in the Bana district.

2 Significance of clay minerals

As was pointed out by Masson (1952), Keller (1968 and 1970), Loughnan (1969), Parham (1969), Pedro (1970), Millot (1970) and Weaver (1989) clay minerals are the most important product as results of weathering. Moreover, mineral species of clay mineral reflect their formation condition and the fact will give us important information for clarifying the weathering condition. Basic igneous rocks are rich in magnesium and are favorable for producing smectite under the condition of poor drainage or low rainfall by weathering but smectite is not found in the Bana complex. However in the case of high rainfall and good drainage such as in the case of the Bana district, magnesium is released from the parent mineral and kaolin minerals will become predominant. Acid igneous rock rich in potassium as well as magnesium are, on the other hand favorable for producing mica clay minerals. Rapid removal of the potash and magnesia from the host rocks leads to the formation of kaolin minerals. As was confirmed in the present research, kaolin minerals are the most abundant clay mineral in the weathered rocks of the Bana complex (Figs. 5, 6 and 7).

The variation of relative amount of clay minerals in the clay fractions obtained in the present research could be reflected the mineralogical transformation during weathering process. The formation process of kaolin minerals can be explained based on the phase diagram show in (Fig. 37). Three stages 1, 2 and 3 are confirmed in the present research. Arrows indicates the path obtained by alteration products. Arrows 2 and 3 show the common reaction in tropical climate where the most intense weathering removes silica from the host rocks producing gibbsite. In weathered Lembo granite, gibbsite is identified coexist with kaolin minerals mostly in the upper part of profile.

For the initial formation of kaolin mineral, feldspar in the host rocks plays an important role. Eggleton and Buseck (1980) concluded that "it is not appropriated to consider reactions occurring simple at the crystal surface ...the beginning of feldspar weathering is, in this instance an equilibrium reaction process leading to the formation of kaolin minerals". Main chemical reactions prevailed during the alteration of feldspar are follows:



Tsuzuki and Kawabe (1983) suggested that dissolution of feldspar plays an important role for reprecipitation of kaolinite. Keller (1978) stated that the most logical mechanism for the production of kaolin-group is via solution. Eswaran and Bin (1978) proposed that feldspar alters via solution to kaolinite and gibbsite, but via a non crystalline stage to halloysite. Typical example of the process is found in the Lembo granite. Formation processes of kaolin minerals in the volcanic and granitic rocks are schematically illustrated in Fig. 38.

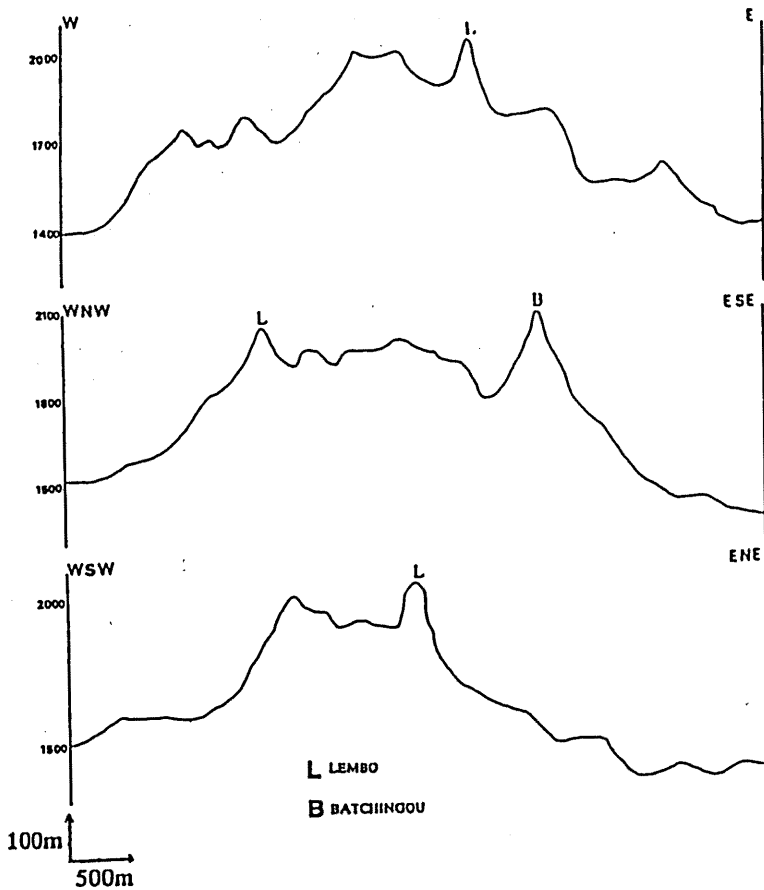


Fig.35 Different topography profiles ar ound the Bana district.

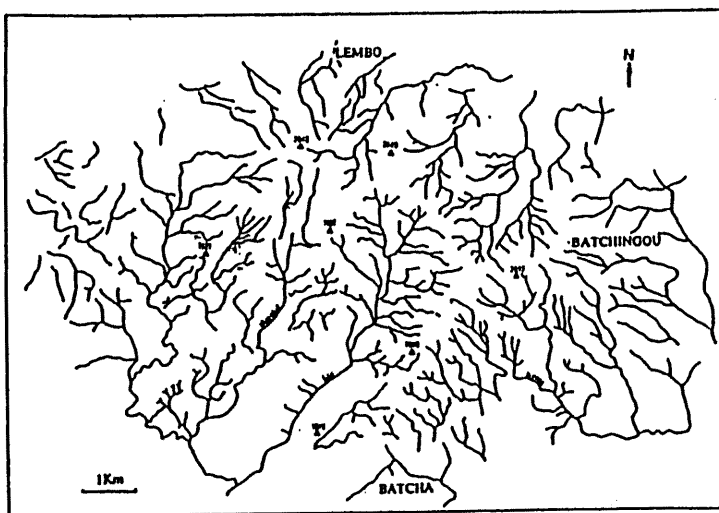


Fig.36 Hydrography network in the Bana district.

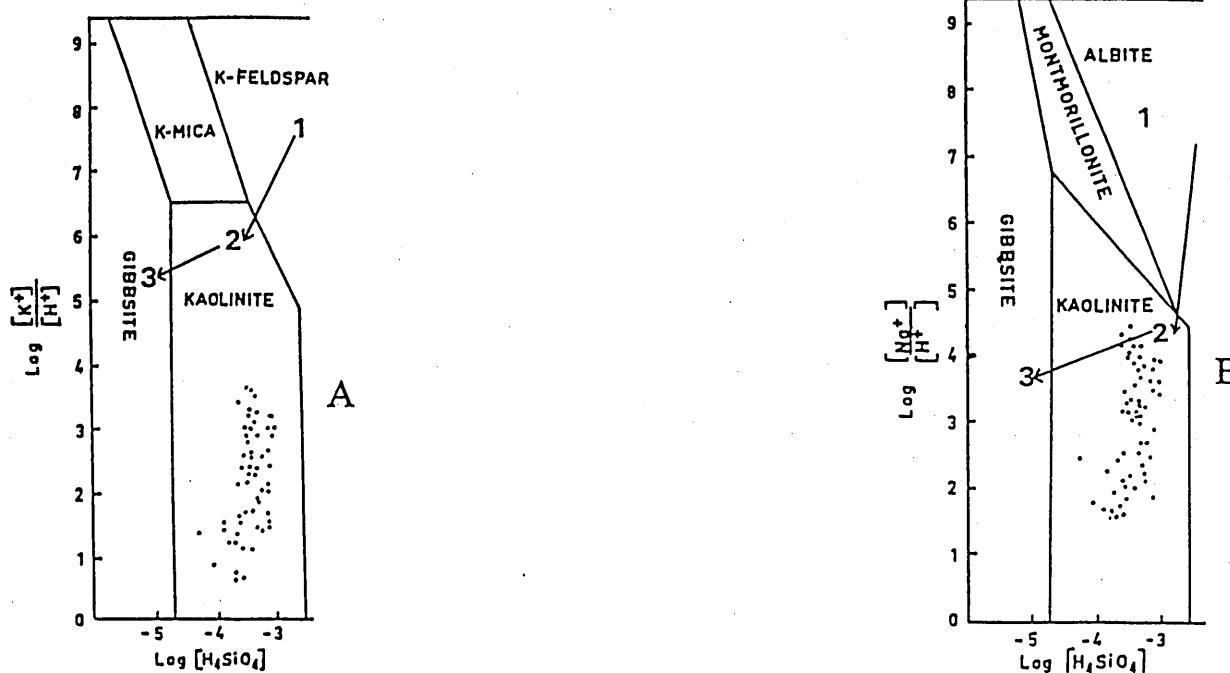


Fig.37 Stability relations of phases in the system A ($K_2O-Al_2O_3-SiO_2-H_2O$) and B ($Na_2O-Al_2O_3-SiO_2-H_2O$) at 25° C and 1 atmosphere total pressure as function of $(K^+)/ (H^+)$, $(Na^+)/ (H^+)$ and (H_4SiO_4) (after Feth et al., 1964)

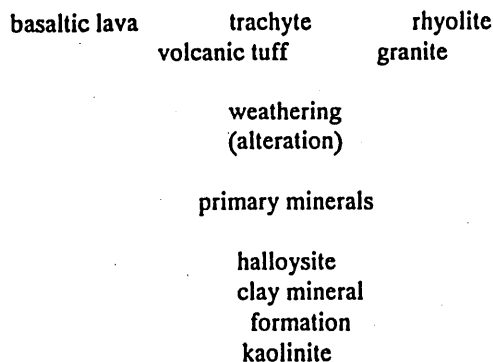


Fig. 38 Weathering sequence of volcanic and granitic rocks of Bana complex.

In the volcanic rocks, the glass weathers readily releasing K, Na and Si and forming alteration product rich in Al, Fe and Ti.

Field observations and mineralogical studies reveal that alteration zones could be distinguished along different profiles of weathered granite and volcanic rocks. The lower zone rich in halloysite with small amount of kaolinite, the middle zone where halloysite and kaolinite are less or more abundant and the upper zone rich in kaolinite. Goethite is observed in the top part with kaolinite in both profiles of weathered Lembo granite and basic volcanics. Nagasawa and Kunieda (1970), reported that kaolinite and halloysite are formed at the upper part and lower parts, respectively of weathering profiles on granite. The common occurrence of both kaolin minerals

is caused by the transformation of halloysite to kaolinite during the weathering process. The mineral sequence established by Parham (1969) at Hong Kong, Eswaran and Bin (1978) in Malaysia is typically found in the Bana complex.

Na^+ , Mg^{++} and Ca^{++} as well as K^+ are readily lost, whereas Si^{4+} is slowly lost. The loss of iron depends on the oxidizing condition during weathering. Al^{3+} is immobile. Nb, Zr, Y and Zn show decreasing tendency whereas Sr, Rb, Pb and Ni show a gain in weathered Lembo granite. In weathered acid volcanic rocks, loss of Sr, Zr, Rb and Zn is recognizable whereas Rb is gained in weathered basic volcanic rocks. Al content in kaolin minerals found in the Bana complex is about 25wt% of Al_2O_3 and the value is less than that of ideal one (39wt%). Ideal kaolin minerals does not contain iron but kaolin minerals of the present research contain several wt% (average Fe is about 5wt%) both in weathered granite and volcanic rocks. The fact suggests that a part of Al in kaolin minerals is substituted by Fe. Formation of kaolinite is evidently favored by acid environment, in which all base elements tend to remove in solution. The Bana kaolin minerals have high Al:Si ratio (1:3) and its formation is promoted by removing silica resulting rich in alumina. It should be mentioned that the formation condition of kaolin minerals described above is also possible for hydrothermal activities. Kitagawa (1989) stressed the significance of clay veins or veinlets in the granitic rocks since the veins are intimately related to the

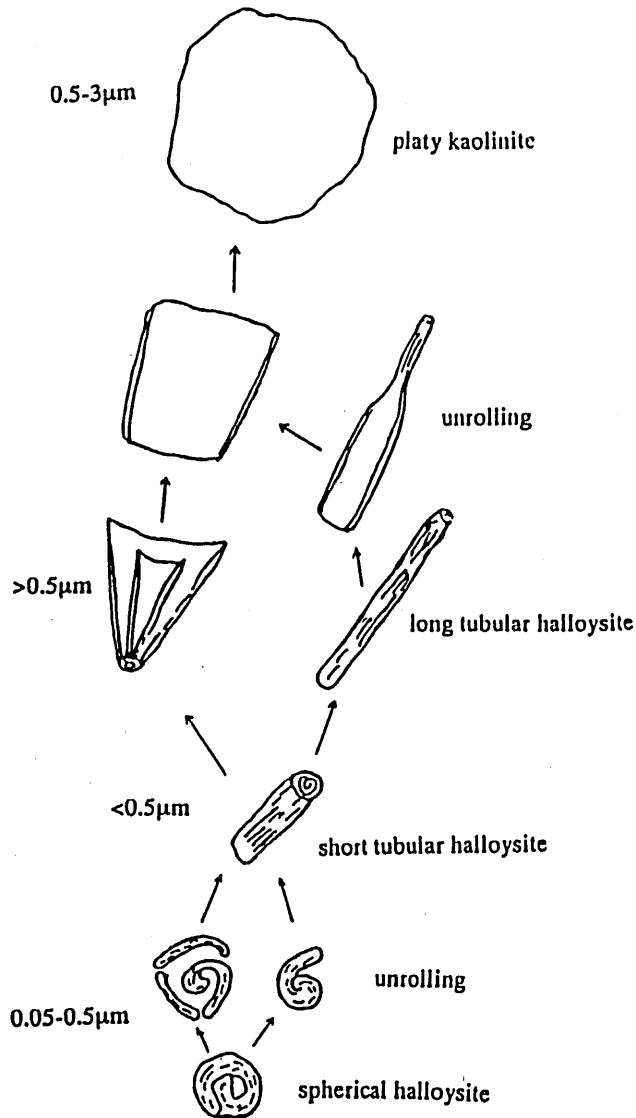


Fig.39 Morphological transformations of the kaolin minerals established in the Bana complex.

hydrothermal activity at the late stage of granitic activity. However, field observation of the Bana complex reveals none of clay veins especially in the granitic rocks. Consequently, the present results are mostly ascribed to weathering.

3 Micro-morphology of kaolin mineral

In the present research, various morphological variation of kaolin crystals were confirmed in the weathered rocks of the Bana complex. These are spherical, short and long tubular, curled and flaky. Among kaolin minerals, halloysite is characteristic in its crystal morphology of tubular form. Formation of the mineral under weathering condition and by hydrothermal activity have been studied by many investigators such as Bates (1962), Parham (1969), Kirkman (1981), Nagasawa (1978a, b). In general tubular and planar curved halloysite are formed from feldspars, whereas spheroidal ones from gel. Nagasawa and Miyazaki (1976) and Nagasawa and Noro (1987) reported that tubular shape is related either to a hydrothermal origin or to biogenic weathering of feldspar in sandy materials. The spheroidal morphology is related to the evolution of allophanic gels (Sudo and Yotsumoto, 1977). Intimate genetical relationship between the size of halloysite and alteration condition (weathering or hydrothermal) are stressed by Kitagawa *et al.*, (1984), Kitagawa and Kameoka (1986) and Kitagawa (1989). That is halloysite of hydrothermal origin mainly show tubular form with narrow width compared with that of weathering. In relation to the fact, Tazaki (1982) and Romero *et al.*, (1992) found that long tubes (length > 1µm) have a lower $\text{SiO}_2/\text{Al}_2\text{O}_3$ ratio compared with that of shorter tubes. Noro (1986) showed that the Fe content increases with the radius of curvature of the tube and reaches maximum in the hexagonal platy halloysite.

As was well confirmed by XRD (Figs. 5, 6 and 7), the constituent minerals of the host rock are remarkably altered to kaolinite and/or halloysite except quartz and K-feldspar. Almost all the clay minerals are considered to be derived from plagioclase in the host rock. The alteration sequence of the kaolin minerals are found in the weathering profiles. That is, in the lower parts halloysite is predominant and kaolinite associated with halloysite is rich in the upper part. Micro-morphologies of the kaolin minerals observed in the present research are schematically represented in Fig. 39. The crystal size of kaolin minerals are intimately related to the variation of morphology. That is, spherical halloysite is in the range of 0.05-0.5µm, short tubular halloysite is less than 0.5µm, long tubular halloysite is over 0.5µm and platy and/or flaky kaolinite is 0.3-3µm. Based on the facts obtained, morphological transformation sequence of single crystal can be reasonably explained in the sequence represented in Fig. 39. Crystal sizes of kaolin minerals grow with morphological transformation. However, whether the morphological transformation of kaolin minerals established in the present research is controlled by the dissolution and neoformation mechanism (Inoue, 1996) or not remains to be solved. The present TEM observation confirms the coarsening of kaolin minerals and the fact suggests that the morphological transformation may probably be controlled by solid transformation process

during weathering.

4 Significance of etch pits.

As was pointed out in the previous, etch pits recorded on crystal surface of resistant minerals such as quartz and K-feldspar provide significant information concerning the nature of the related solutions.

From SEM observation, commonly developed etch pits and various dissolution patterns on quartz and K-feldspar grain surface were confirmed in the present study. These are triangular pits, irregular solution pits, precipitated plates and deep grooves. These morphologies are comparable with chemical dissolution pits reported by Wilson (1978). Moreover, the obtained patterns are closely similar to those from kaolin deposits of weathering origin such as Tirschenreuth in Germany and Elena in Russia (Kitagawa and Koster, 1991; Kitagawa *et al.*, 1994). What can be said is that, number of etch pits surely increases as weathering proceeds. Moreover, the complicated morphology strongly suggests that the weathering condition was not monotonous but various conditions such as pH and micro-environments. Establishment of systematic morphological sequence in relation to chemical characteristics such as pH together with temperature will give us important and more detailed information concerning the micro-environment during the weathering process.

VI. CONCLUSION

Weathering process of various igneous rocks composed of the Bana complex in western Cameroon were investigated. The Bana complex is composed of mainly granite, basalt, trachyte and rhyolite. All of these rocks are weathered extensively under the tropical humid and arid climate. The constituent minerals of the host rock as well as weathered rocks were examined in detail under microscope and by means of XRD, XRF and electron microscope (SEM and TEM) together with electron microprobe analyses.

XRD analyses reveals that kaolin minerals are the most common weathering products through out the district and regardless the rock type. Some typical weathering profiles were selected in the Bana complex and the detailed mineralogical examination confirms the alteration sequence of clay minerals. The established mineralogical sequence was further confirmed by morphological variations of kaolin minerals observed using SEM method. Etch pits developed on quartz and K-feldspar surface were also investigated and the result shows that quartz and K-feldspar surfaces of the upper parts are much rougher than those of the lower parts. The fact suggests that the upper parts are more suffered to weathering than lower parts. The variation of number and size of etch pits obtained suggests the variation of pH and the value is controlled by respective microenvironment.

The mode of occurrence of halloysite in the lower part together with its characteristic morphology suggests that halloysite is the earlier weathering product derived from feldspars and glasses and the mineral evolves crystallographically into kaolinite with increasing weathering process. This is confirmed by the micro-morphology of kaolin minerals found in the Bana complex. The possible pathway of clay minerals within the profiles

in the Bana district is as follows: spherical halloysite-short tubular halloysite - long tubular halloysite - platy kaolinite.

Table.1. Annual rainfall in west Cameroon

	BAFOUSSAM	BAFANG (BANA)	BANGANGTE	DSCHANG	NKOUNDJA	BAMENDA
Years	mm	mm	mm	mm	mm	mm
1970	1691.7	1879.9	1394.6	1613.5	2054.5	2167.8
1971	1900.8	1980.9	1275.7	2168.9	1950.4	1978.8
1972	1881.9	1526.2	1166.1	1570.6	1726.6	2143.6
1973	1639.4	1455.1	1368.0	1413.3	1828.8	1947.7
1974	1844.9	1961.7	1377.7	2109.2	2118.8	2414.3
1975	1861.8	1744.6	1305.4	1819.8	2125.5	2205.1
1976	2133.3	2054.8	1363.1	2438.5	2121.5	2587.9
1977	1685.1	1643.2	1435.8	2034.5	1661.6	2209.8
1978	1583.3	2022.8	1438.6	1904.9	2016.0	2464.0
1979	1763.7	1438.8	1250.3	1707.7	2102.7	2718.3
1980	1785.4	1659.6	1201.2	1856.4	2093.3	2502.4
1981	1643.7	1806.8	1168.8	1814.4	1988.3	2504.9
1982	2081.4	1875.9	1377.8	2232.2	2127.6	2377.0
1983	1336.9	1506.6	1134.8	1596.5	1379.1	2179.2
1984	1525.0	1603.6	1342.4	1636.6	1816.6	2299.7
1985	2044.4	1920.0	1582.8	1764.6	1950.0	2267.4
1986	1611.2	2049.7	1395.4	1819.4	1844.3	2210.1
1987	1519.4	1872.2	993.5	1779.1	1653.3	1795.1
1988	1771.8	1894.8	1246.1	1795.2	1541.1	2107.1
1989	1664.7	1784.1	1177.7	1588.6	2082.8	2297.1
1990	1864.4	2191.2	1276.3	1734.7	1824.5	2427.4
1991	1730.4	1861.1		1413.7	1799.5	2197.4
1992	1957.1	2238.0		1750.6	1925.4	2520.7
1993	2070.1	1937.0		1852.4	2069.1	2522.1
1994	1871.9	1881.0		1748.7	1448.4	2429.3
1995		1550.0		1748.6		2123.0

(Source: Weather bureau-Ministry of Transport-Cameroon)

REFERENCES

- Aagaard, P. and Helgeson, H. C. (1982) Thermodynamic and kinetic constraints on reaction rates among minerals and aqueous solution: I. Theoretical considerations: *Amer. J. Sci.* 282, 237-285.
- Al-Saleh, S. and Khalaf, F. I. (1982) Surface textures of quartz grains from various recent sedimentary environments in Kuwait. *Jour. Sediment. Petrol.* 52, No. 1, 215-225.
- Anand, R. R., Gilkes, R. J., Armitage, T. M., and Hillyer, J. W. (1985) Feldspar weathering in lateritic saprolite. *Clays and Clay Minerals*, Vol. 33 No. 1, pp. 31-43.
- Banfield, J. F. and Eggleton, R. A. (1990) Analytic transmission electron microscope studies of plagioclase, muscovite, and K-feldspar weathering. *Clays and Clay Minerals*. 38, 77-89.
- Bates, T. F., Hildebrand, F. A., and Swineford, A. (1950) Morphology and structure of endellite and halloysite. *Amer. Mineral.* 6, 237-248.
- Bates, T. F. (1962) Halloysite and gibbsite formation in Hawaii. *Clays and clay Minerals* 9, 315-328. in mineralogical properties of halloysite as related to its genesis. *Proc. Inter. Clay conf.* 1975 Nagasawa and Miyazaki.
- Berner, R. A. and Holdren, G. R. (1977) Mechanism of feldspar weathering: some observation evidence. *Geology* 5, 369-372.
- Berner, R. A., and Holdren, G. R. (1979) Mechanism of feldspar weathering. II. Observations of feldspars from soils. *Geochim Cosmochim Acta* 43, 1173-1186.
- Bird, M., Fyfe, B., Chivas, A. and Longstaffe, F. (1990) Deep weathering at extra-tropical latitudes: a response to increased atmospheric CO₂, soils and Greenhouse effect. ed. A. F Bouwman, John Wiley & Sons Ltd., 382-389.
- Blum, A. E. and Stillings, L. L. (1995) Feldspar dissolution kinetics. *Reviews in mineralogy*. Vol. 31, 291-342.
- Caen, V. M., Tempier, P., Nana, J. M. (1991) Le granite de Lembo (partie du complexe volcano-plutonique de Bana), témoin du magmatisme tertiaire du Cameroun. *Geochronologie. Bull. Soc. Geol. Fr.* No. 3, 497-501.
- Calvert, C. S., Buol, S. W. and Weed, S. B. (1980) Mineralogical characteristics and transformations of a vertical rock-saprolite-soil sequence in the north Carolina Piedmont-profile morphology, chemical composition and mineralogy. *Soil. Sc. Soc. Am. Jour.* 44, 1093-1103.
- Churchman, G. T., Whitton, J. S., Claridge, G. G. C., and Theng, B. K. G. (1984) Intercalation method using formamide for differentiating halloysite from kaolinite. *Clays and Clay Minerals*. 32, 241-248.
- Delvaux, B., Herbillon, A. J., and Vielvoye, L. (1989) Characterization of a weathering sequence of soils derived from volcanic ash in Cameroon. Taxonomic, mineralogical and agronomic implications: *Geoderma* 45, 375-388
- Dixon, J. B. and Mc Kee, T. R. (1974) Internal and external morphology of tubular and spheroidal halloysite particles. *Clays and Clay Minerals* 22, 127-137.
- Dixon, J. B. (1977) Kaolinite and serpentinite group minerals pp357-403 in: *Minerals in soil environments* (J. B. Dixon & S. B. Weed, editors). *Soil Sci. Soc. Am., Madison, Wisconsin.*
- Dumort, J. C. (1968) Notice explicative sur la feuille Douala-Ouest avec carte géologique au 1/500. 000. *Imp. Nat. Yaounde. Cameroun.* 60 p.
- Eggleton, R. A., and Busseck, P. R. (1980) High resolution electron microscopy of feldspar weathering. *Clays and Clay Minerals*. Vol. 28, No. 3, 173-178.
- Eswaran, H., and Bin, W. C. (1978) A study of deep weathering profile on granite in peninsular Malaysia: III. Alteration of feldspars. *Soil. Sci. Soc. Amer. Jour.* 42, 154-158.
- Feth, J. H., Robertson, C. E., and Polzer, W. L. (1964) Source of mineral constituents in water from granitic rocks, Sierra Nevada, California and Nevada, U. S. Geol. Surv. Water Supply Paper 1535-I. In *Chemical weathering of silicate minerals*. Loughnan, F. C.
- Fund, P. C., and Sanipelli, G. G. (1982) Surface studies of feldspar dissolution using surface replication combined with electron microscope and spectroscopic techniques. *Geochim Cosmochim Acta*. Vol. 46, 503-512.
- Gazel, J., Lasserre, M., Limasset, J. C., et Vachette, M. (1963) Age absolus des massifs granitiques ultimes et la minéralisation en étain du Cameroun occidental. *C. R. Acad. Sci. Fr.* Vol. 256, 2875-2878.
- Geze, B. (1941) Les massifs volcaniques du Cameroun occidental. *C. R. Acad. Sci. Fr.* 212 No 12, 498p.
- Geze, B. (1943) Géographie physique et géologique du Cameroun occidental. *Mem. Mus. National Hist. Natur. Paris N. Se.* 17, 1-272.

- Giret, A; Bonin, B; and Leger, J. M. (1980) Amphibole compositional trends in oversaturated and undersaturated alkaline plutonic ring-complexes. *Can. Miner.* Vol. 18, 481-495.
- Ghogomu, T. R. (1984) Geology, geochemistry and petrology of the Ntumbay anorogenic complex, Cameroon, an example of a ring-complex of intermediate composition. Thesis. Univ of Nancy I. 142 p.
- Glassman, J. R. and Simonson, G. H. (1985) Alteration biotite in soils of western Oregon. *Soil Science Society of America, Jour.*, 46, 17-58.
- Goldich, S. S. (1938) A study of rock weathering, *J. Geol.* 46, 17-58
- Gouhier, J., Nougier, J., et Nougier, G. (1974) Contribution a l'etude volcanologique du Cameroun ("ligne du Cameroun"-Adamaoua). *Ann. Fac. Sc. Uni. Yde* 17, 3-18.
- Heier, K. and Adams, J. A. (1964) The geochemistry of metals. *Phys. Chem. Earth*;5, 253-382.
- Holdren, G. J., and Berner, R. A. (1979) Mechanism of feldspar weathering I. Experimental studies. *Geochim. Cosmochim. Acta.* Vol. 43, 1161-1171.
- Inoue, A. (1996) Solution-mediated phase transformations of clay minerals. *Jour. Mineral. Soci. Japan*, 25, 4, 189-197.
- Jenny, H. (1941) Factors in soil formation. Mc Graw-Hill, New York.
- Keller, W. D. (1957) Principles of chemical weathering. Columbia, Missouri. 111 p.
- Keller, W. D. (1968) Flint clay and flint-clay facies: *Clays and Clay Minerals* 16, 113-128
- Keller, W. D. (1970) Environmental aspects of clay minerals. *Jour. Sed. Petrol.* 40, 788-813.
- Keller, W. D. (1976a) Scanning electron micrographs of kaolins collected from diverse environments of origin-1. *Clays and Clay Minerals.* 24, 107-113.
- Keller, W. D. (1976b) Scanning electron micrographs of kaolins collected from diverse environments of origin-2. *Clays and Clay Minerals.* 24, 114-117.
- Keller, W. D. (1977) Scanning electron micrographs of kaolins collected from diverse environments of origin. V. Kaolins collected in Australia and Japan on field trips of the sixth seventh clay conferences: *Clays and Clay Minerals*, 25, 345-364.
- Keller, W. D. (1978a) Progress and problems in rock weathering related to stone decay. In E. M. Winkler (Editor). *Engineering Geology Case, Histories* Number 11. *Geol. Soc. Amer.* 37-46.
- Keller, W. D. (1978) Kaolinization of feldspar as displayed in scanning electron micrographs. *Geology*, 6, 184-188.
- Keller, W. D. (1989) Scanning electron micrographs of clay minerals formed by weathering and other genetic processes. pp. 29-47. In *weathering, its products and deposits*. Vol. 1. Theophrastus Publication, SA.
- Kirkman, J. H. (1977) Possible structure of halloysite disks and cylinders observed in some New-Zealand rhyolitic tephra: *Clay Miner.* 12, 199-216.
- Kirkman, J. H. (1981) Morphology and structure of halloysite in New Zealand Tephra. *Clays and Clay Minerals*, 29, 1-9.
- Kitagawa, R. and Kakitani, S. (1977) Alteration of plagioclase in granite during weathering. *Jour. Sci. Hiroshima Univ., Seri. C*, 7, 4, 183-197.
- Kitagawa, R., Hirosawa, H., Nagai, K., and Nobushita, T. (1984) The shape and genesis of halloysite formed by alteration of granitic and rhyolitic rocks. *Jour. Clay Sci. Soc. of Japan*, vol. 24, 20-33.
- Kitagawa, R. and Kameoka, H. (1986) The mode of occurrence and mineralogy Komaki halloysite and alteration of its surrounding granitic rock. *J. Clay Sci. Soc. Japan*, 26, 78-89.
- Kitagawa, R. (1989) Clay veins and clay minerals in the granitic rocks in Hiroshima and Shimane Prefectures, southwest Japan. - Effect of the hydrothermal activities on the decomposition of the granitic rocks. *Jour. Sci. Hiroshima Uni., Ser. C*. 8, 47-80.
- Kitagawa, R., and Koster, H. M. (1991) Genesis of the Tirschenreuth Kaolin deposit in Germany compared with the Kohdachi kaolin deposit in Japan. *Clay Minerals* 26, 61-79.

- Kitagawa, R., Koster, H. M., Yeon, H. J. (1994) Scanning electron microscope examination of quartz surface textures from kaolinized granitic rocks. *Jour. Scie. Hiroshima Univ., Ser. C, Vol. 10, No. 1, 159-172.*
- Krinsley, D., and Cavallero, L. (1970) Scanning electron microscopy examination of periglacial eolian sand from island, New York. *Jour. Sed. petrol. 40, 1345-1350.*
- Krinsley, D. H., and Doornkamp, J. C. (1973) *Atlas of quartz sand surfaces textures: London, Cambridge Univ. Press, 91.*
- Kurahayashi, S., and Tsuchiya, T. (1960) On the clay minerals of the Kanto Loam(3). *Geol. Soc. Japan J., 66, 586-593 (in Japanese, with English abstract).*
- Laird, J. and Albee, A. L. (1981) Pressure, temperature, and time indicator in mafic schist: Their application to reconstructing the polymetamorphic history of Vermont. *Amer. J. Sci. 281, 127-175.*
- Lasaga, A. C. (1981) Rate laws of chemical reactions: in kinetic of geochemical processes, review in mineralogy Vol. 8, A. C. Lasaga and R. J. Kirkpatrick, eds., Mineral. Soc. Amer., Washington, D. C. 1-68.
- Lasaga, A. C., Soler, J. M., Ganor, J., Burch, T. E., and Nagy, K. L. (1994) Chemical weathering rate laws and global geochemical cycles. *Geochim. Cosmochim. Acta 58, 2361-2386.*
- Lasserre, M. (1966) Confirmation de l'existence des granites tertiaires au Cameroun (Afrique equatoriale). *Bull. B. R. G. M. Fr. No. 3, 141-148.*
- Lasserre, M. (1978) Mise au point sur les granitoides dits "ultimes" du Cameroun: gisement, petrographie et geochronologie. *Bull. B. R. G. M. sect IV. No. 2, 143-156.*
- Leake, B. E. (1978) Nomenclature of amphibole. *Miner. Magazine. Vol. 42, 553-563*
- Loughnan, F. C., and Bayliss, P. (1961) The mineralogy of bauxite deposits near Weipa, Queensland, Am. *Mineralogist 46, 209-217.*
- Loughnan, F. C. (1969) Chemical weathering of the silicate minerals. Elsevier, New York, 154 p.
- Masson, B. (1952) Principles of geochemistry. Third edition N. Y 329 p.
- Millot, G. (1970) Geology of clays. Springer-Verlag, N. Y., 429 p.
- Moreau, C. (1978) Mise en evidence sur photographie satellite ERTS d'elements structuraux dans l'Air central. 26 eme Congr. Inter. Geol. Paris. t. 1. fasc. 1, 21-23.
- Morin, S. (1980) Apport des images Landsat a la connaissance de la structure des hautes terres de l'ouest Cameroun. *Geogr. phys. Dept. Geog. Yaounde, 181-196.*
- Nagasawa, K. (1969) Kaolin minerals in Cenozoic sediments of Central Japan, Proc. Intern. Clay Conf., Tokyo 1, 15-30.
- Nagasawa, K. and Kunieda, K. (1970) Geology and mineralogy of clay deposits in the Naegi district, Gifu prefecture, *Mining Geol., 20, 6, 361-377.*
- Nagasawa, K. and Miyazaki, S. (1976) Mineralogical properties of halloysite as related to its genesis: in proc. 6th Int. Conf. Mexico city, 1975, S. W. Bailey, ed., Wilmette, Illinois, 256-265.
- Nagasawa, K. (1978a) Weathering of volcanic ash and other pyroclastic material. pp 105-125 in *Clays and Clay Mineral in Japan (Sudo & Shimoda, editors). Kondansha, Tokyo/Elsevier, Amsterdam.*
- Nagasawa, K. (1978b) Kaolin minerals. 189-219 in *Clays and Clay Minerals of Japan (Sudo & Shimoda, editors). Kondansha, Tokyo, Elsevier, Amsterdam.*
- Nagasawa, K. and Noro, H. (1987) Mineralogical properties of halloysites of weathering origin. *Chem. Geol. 60, 145-149.*
- Nana, J. M. (1988) Le complexe volcano-plutonique de Bana (Ouest-Cameroun): Geologie et petrologie. These. Univ. de Paris-Sud (Centre d'Orsay). 131 p.
- Ngonge, E. D. (1988) A geological study of the anorogenic complex of Guenfalabo (an example of a complete series) in the region west of Adamawa highlands. Thesis. Univ. Yaounde. Fac. Sci. 156 p.
- Nkombo, C. (1990) Etude geologique des Monts Roumpi: un ensemble plutonic et volcanique de la "Ligne du Cameroun". These de doctorat. Univ. de Nancy I. 352 p.
- Nna, O. (1975) L'alteration des roches volcaniques dans les Monts Bamenda, Cameroun: geologie, mineralogie, geochemie these 3eme cycle Uni. Paris VI. 109 p.
- Nono (1987) Petrologie d'un volcan alcalin intraplaque: le massif de Nghanha dans l'Adamaoua (Cameroun). These de doctorat. Univ. de Nancy I. 158 p.

- Noro, H. (1986) Hexagonal platy halloysite in altered tuff bed, Komaki City, Aichi Prefecture, central Japan: *Clay Miner.* 21, 401-415.
- Okada, S. (1973) Clay minerals in the Shikotsu pumice fall deposits. *Geol. Soc. Japan.*, 79, 363-375. (in Japanese, with English abstract).
- Parham, W. E. (1969) Halloysite-rich tropical weathering product of Hong Kong. *Proc. Internat. Clay. Conf. Tokyo* 1, 403-416.
- Pedro, G. (1966) Essai sur la caracterisation geochemique des differents processus zonaux resultant de l'alteration superficielle. *C. R. Acad. Sci. Paris*, 262D, 1828-1831.
- Pedro, G., Berrier, J., Tessier, D. (1970) Recherches experimentales sur l'alteration "allitique" des argiles dioctaedriques de type kaolinite et illite. *Bull. Gr. Ev. Argiles t. XXII*, 29-50.
- Poldervart, A. and Hess, H. H. (1951) Pyroxene in the crystallization of basaltic magma. *Journ. Geol.*, 59, 472-489.
- Pomerol, C. and Fouet, R. (1969) Les roches eruptives in P. U. F Paris. 91-123.
- Quantin, P. (1990) Specificity of the halloysite rich tropical or subtropical soils. *Trans. 14th Int. Congr. Soil Sci.*, Kyoto, 16-21.
- Quantin, P. (1991) Les sols de l'archipel volcanique des nouvelles-Hebrides (Vanuatu). Etude de la pedogenese initiale en milieu tropical. These, U. E. R. des Sciences de la Vie et de la Terre, Institut de Geologie, Strasbourg.
- Robertson, J. D. M. and Eggleton, R. A. (1991) Weathering of granitic muscovite to kaolinite and halloysite and of plagioclase-derived kaolinite to halloysite. *Clays and Clay Minerals* 39, 113-126.
- Romero, R., Robert, M., Elsass, F. and Garcia, C. (1992) Abundance of halloysite neof ormation in soils developed from crystalline rocks. Contribution of transmission electron microscopy. *Clay Minerals*, 27, 35-46.
- Sand, L. B. (1956) On the genesis of residual kaolins. *Am. Min.* 41, 28-40.
- Schneider, H. E. (1970) Problems of quartz grain morphoscopy. *Sedimentology*, 14, 325-335.
- Siffermann, G. and Millot, G. (1969) Equatorial and tropical weathering of recent basalts from Cameroon: Allophanes, halloysite, meta-halloysite, kaolinite and gibbsite. *Inter. National Clay Conf. Tokyo* 1, 417-430.
- Sudo, T., and Yotsumoto, M. (1977) The formation of halloysite tubes from spheritic halloysite. *Clays and Clay Minerals*, 25, 155-159.
- Tardy, Y., Bocquier, G., Paquet, H. and Millot, G. (1973) Formation of clay from granite and its distribution in relation to climate and topography. *Geoderma*, 10, 271-284.
- Tazaki, K. (1982) Analytical electron microscopic studies of halloysite formation processes. Morphology and composition of halloysite. *Proc. Int. Clay conf. Bologna-Pavia*, 573-584.
- Tazaki, K. and Fyfe, W. S. (1987) Primitive clay precursors formed on feldspar. *Can. J. Earth Sci.* 24, 506-527.
- Tchawa, P. (1991) Dynamique des paysages sur la retombee meridionale des hauts plateaux de l'Ouest Cameroun. These, de doctorat. Universite de Bordeaux III. 209 P.
- Tchoua, M. F. (1974) Contribution a l'etude geologique et petrologique de quelques volcans de la ligne du Cameroun (Mount Manengouba et Bamboutos). These Doct. d'etat. Univ. Clermont Ferrand. 347 p.
- Tempier, P., Lasserre, M., Sabourdy, G. (1981) Les granitoides panafricains du Nord Cameroun: petrographie et geochemie. *Bull. Soc. Geol. Fr.*, 7, t. XXIII, No. 6, 335-360.
- Theng, B. K. G., Churchman, G. J., Whitton, J. S., and Claridge, G. G. C. (1984) Comparison of intercalation methods for differentiating halloysite from kaolinite. *Clays and Clay Minerals*, 32, 4, 249-258.
- Tsuzuki, Y. and Kawabe, I. (1983) Polymorphic transformation of kaolin minerals in aqueous solutions: *Geochim. Cosmochim. Acta* 47, 59-66.
- Velde, B. (1985) Clay minerals. A physico-chemical explanation of their occurrence. *Developments in sedimentology* 40 Elsevier 427 p.
- Weaver, C. E. (1989) Clays, Muds, and Shales. *Developments in sedimentology* 44 Elsevier. 819 p.
- Wilson, P. (1978) A scanning electron microscope examination of quartz grain surface textures from the weathered millstone grit (Carboniferous) of the Southern pennis, England. A preliminary report. 319-328.
- Wollast, R. (1967) Kinetics of the alteration of K-feldspar in buffered solutions at low temperature: *Geochim. Cosmochim. Acta* 31, 635-648.

WOOATONG Armand S.L.
 Department of Earth Science, Faculty of Science, University of Dschang.
 p.o Box 67, Dschang-Cameroon

EXPLANATION OF PLATES

- Plate 1-SEM micrograph showing different dissolution etch pits from the lower part to the upper part (A, B, C, D) on quartz grains.
- Plate 2-SEM micrograph showing different dissolution etch pits on K-feldspar grains from the lower part to the upper part (A, B, C, D).
- Plate 3-SEM micrograph showing rectangular shape etch pits and conical hollow developed on the K-feldspar (A, B).
- Plate 4-SEM micrograph showing different morphologies of halloysite (A, B) (smooth surface of halloysite) and kaolinite (C, D) (stack of book of platy kaolinite)
- Plate 5-SEM micrograph of aggregation texture of kaolinite. A: showing skeletal matrix texture, B: a coating of fine granule materials on the surface of particles, C: showing porous skeletal matrix texture and vertical section of parallel clay particles, D: showing randomly oriented cluster contact texture.
- Plate 6-TEM micrograph of different morphologies of clay mineral in specimens collected from weathered Lembo granite. A and B: showing spherical and short tubular halloysite, C: showing short tubular halloysite, D: showing platy kaolinite.
- Plate 7-TEM micrograph of different morphologies of clay mineral in specimens collected from weathered basic volcanic rocks. A: showing spherical and short tubular halloysite, B: showing long tubular halloysite, C: showing goethite with amorphous, D: showing platy kaolinite with amorphous.
- Plate 8-TEM micrograph of different morphologies of clay mineral in specimens collected from weathered acid volcanic rocks. A: showing spherical and tubular halloysite, B: showing wide tubular halloysite, C: showing thin tubular halloysite, D: showing thin tubular halloysite and platy kaolinite.

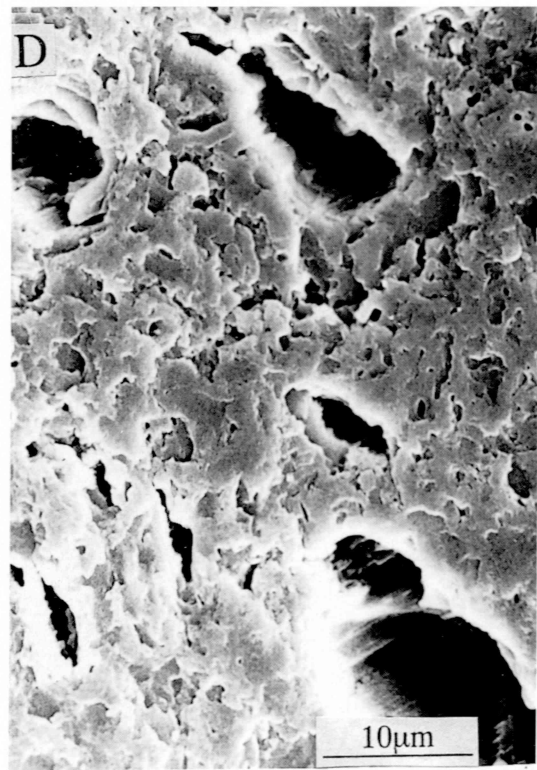
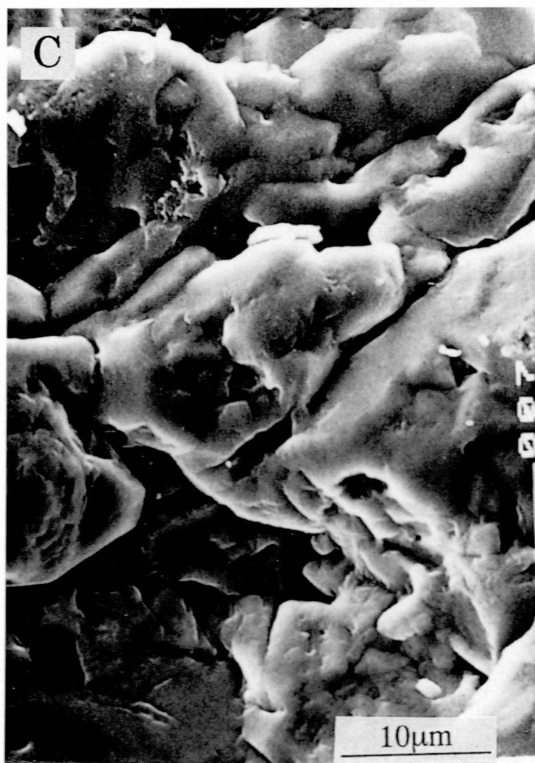


Plate 1

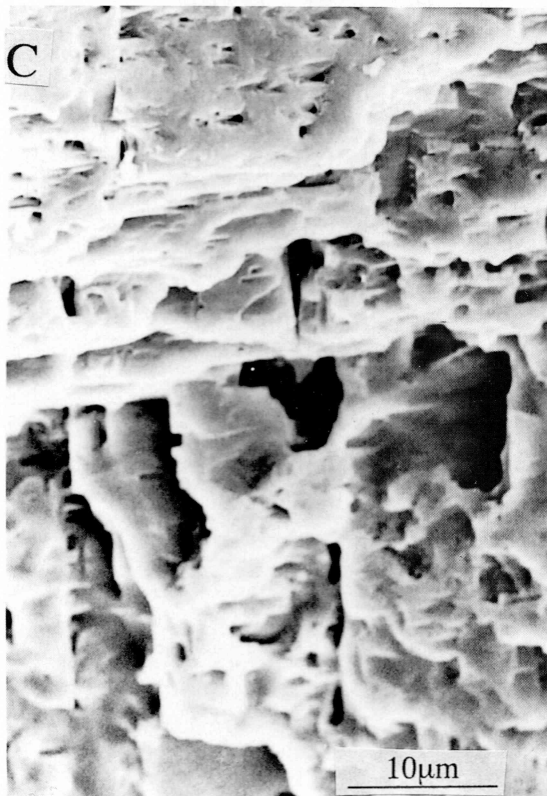
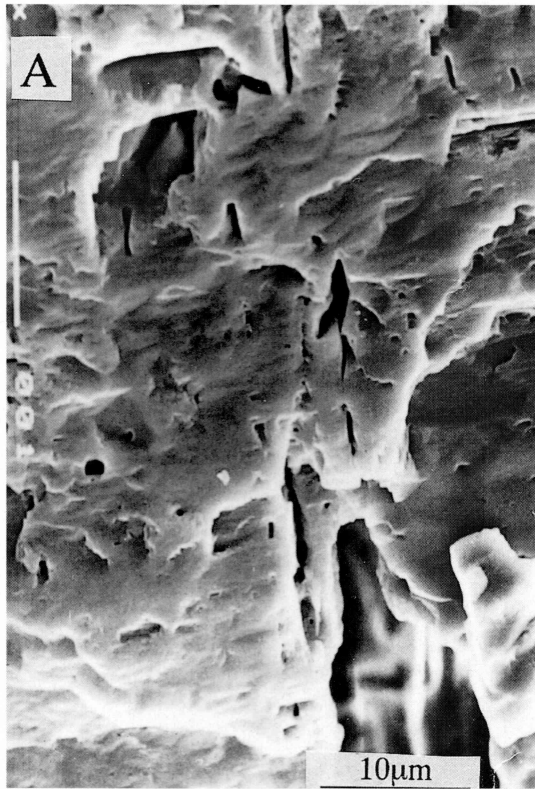


Plate 2

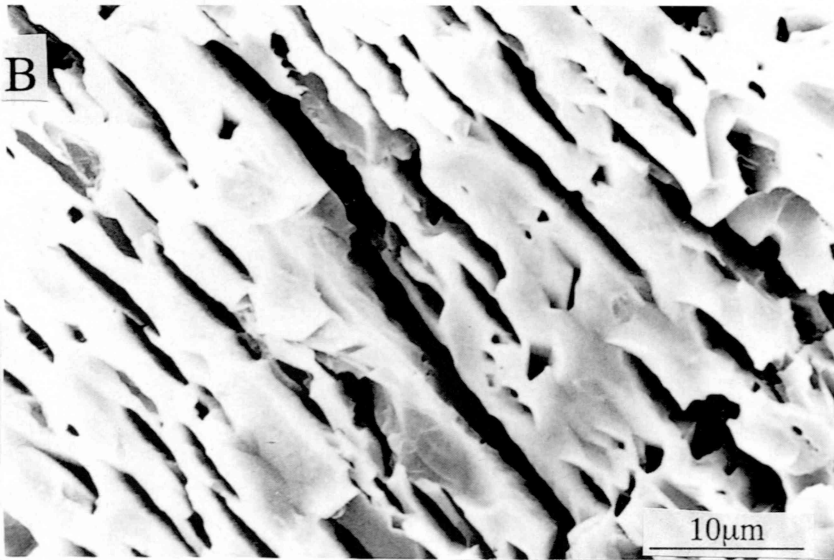
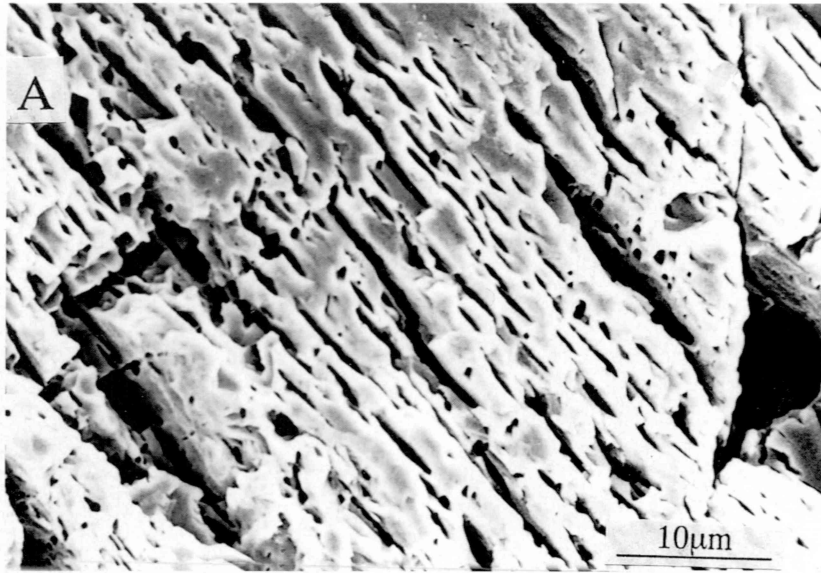


Plate 3

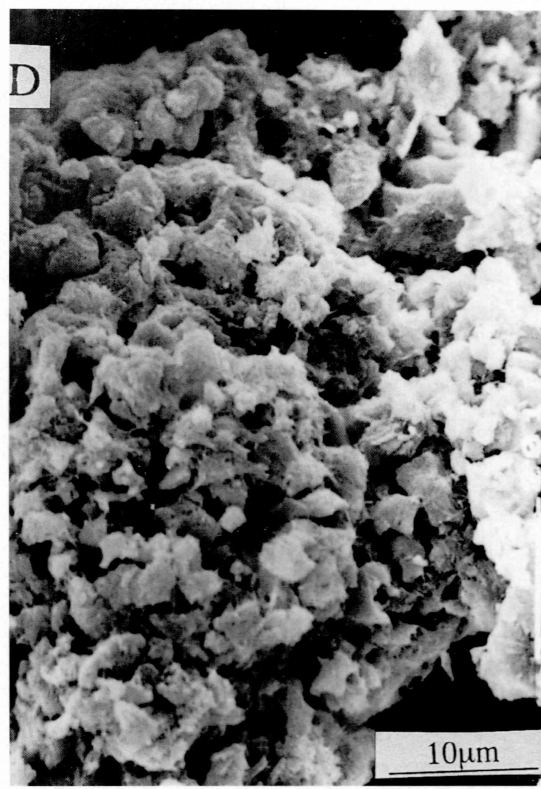
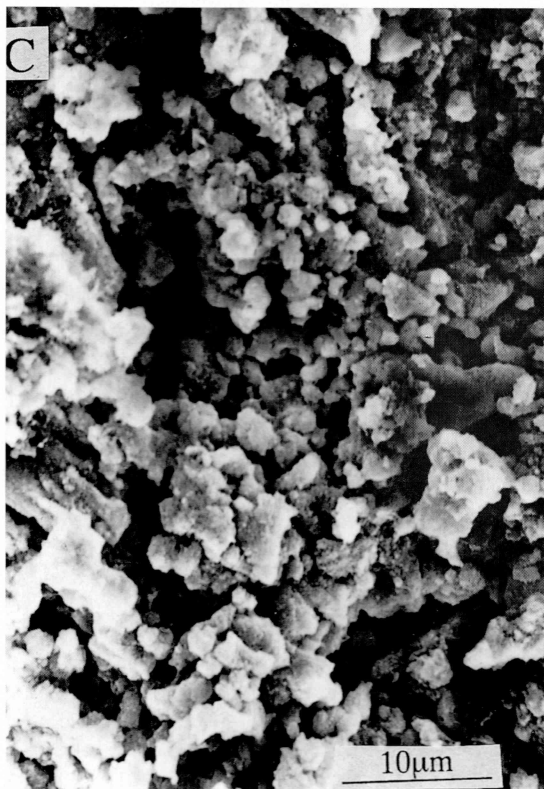
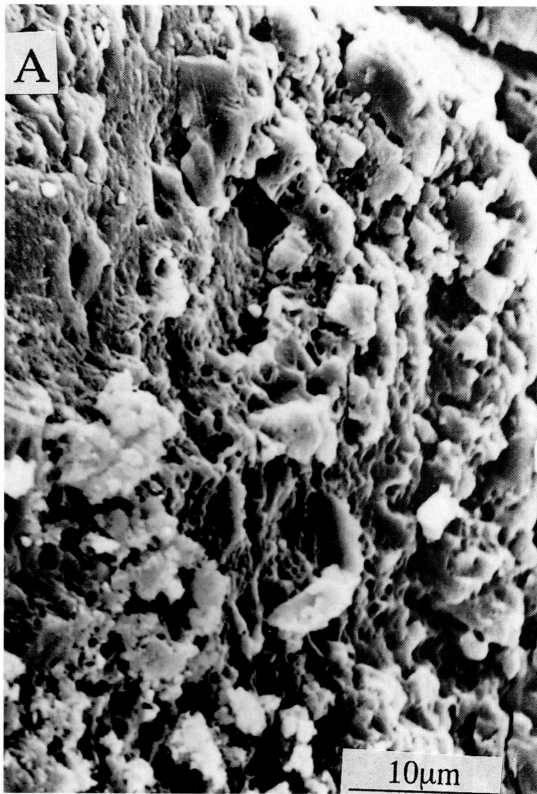


Plate 4

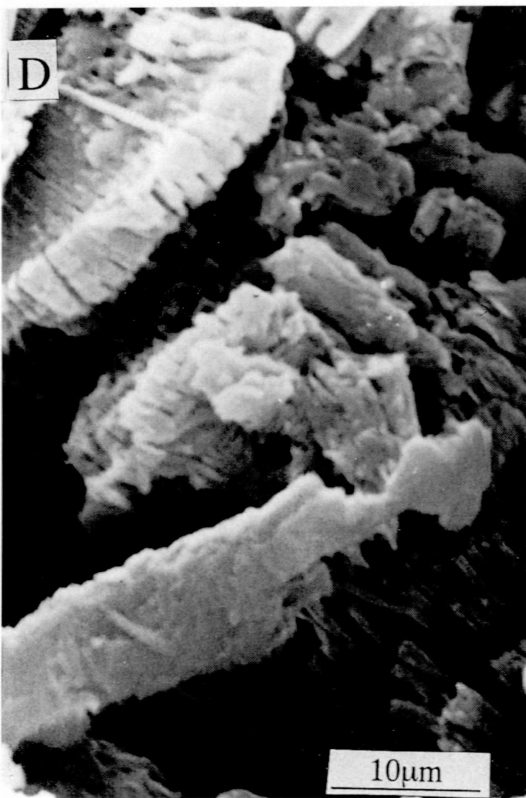
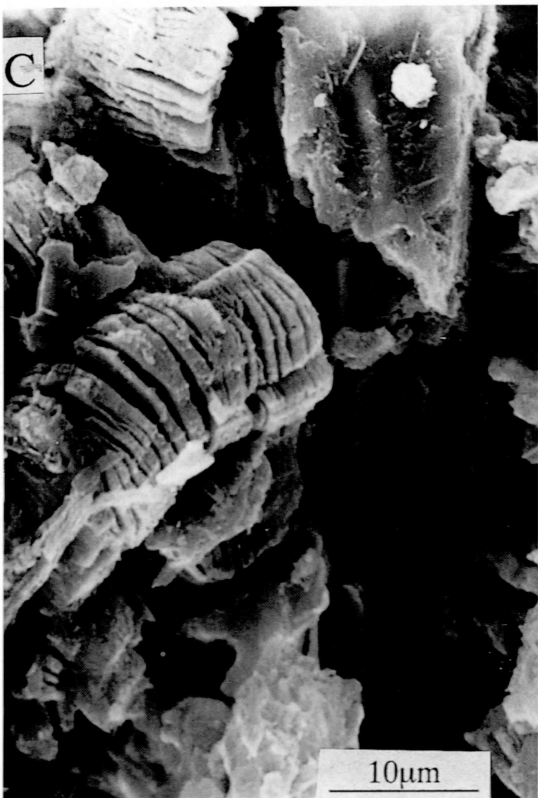


Plate 5

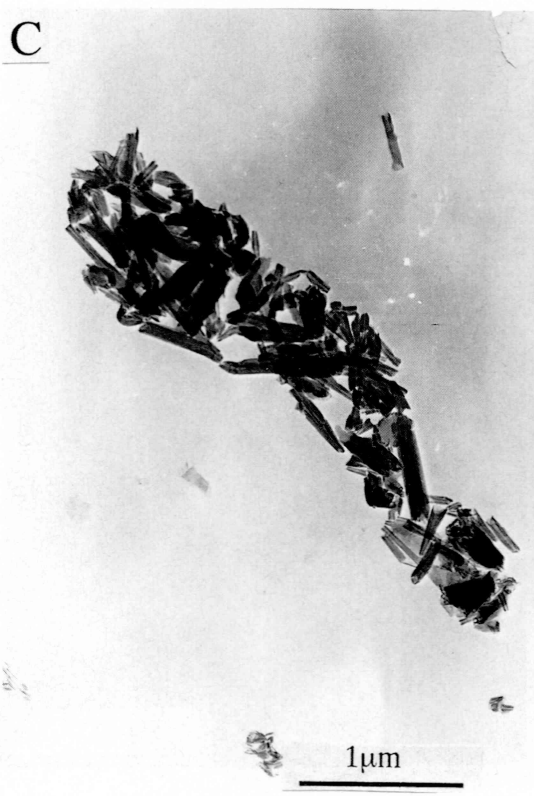
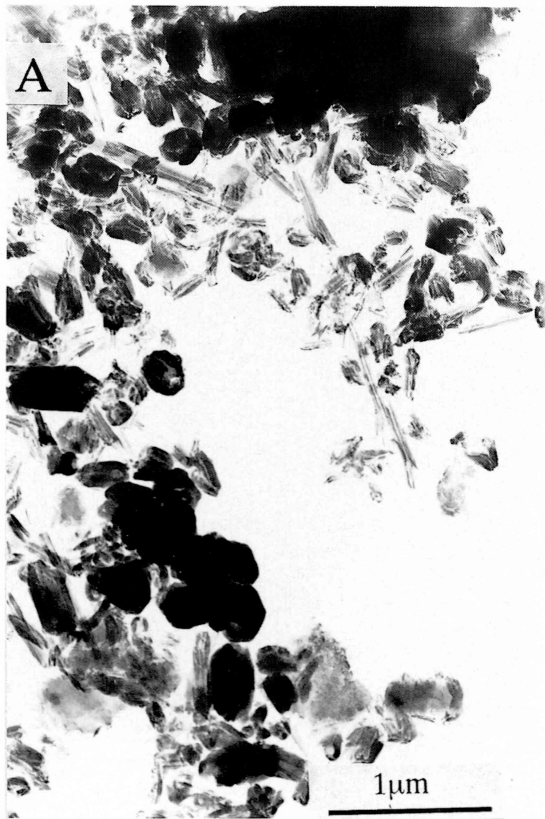


Plate 6

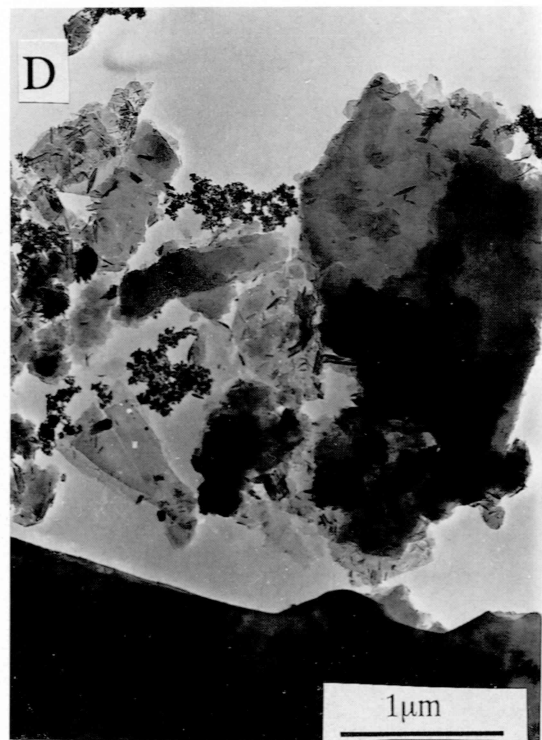


Plate 7

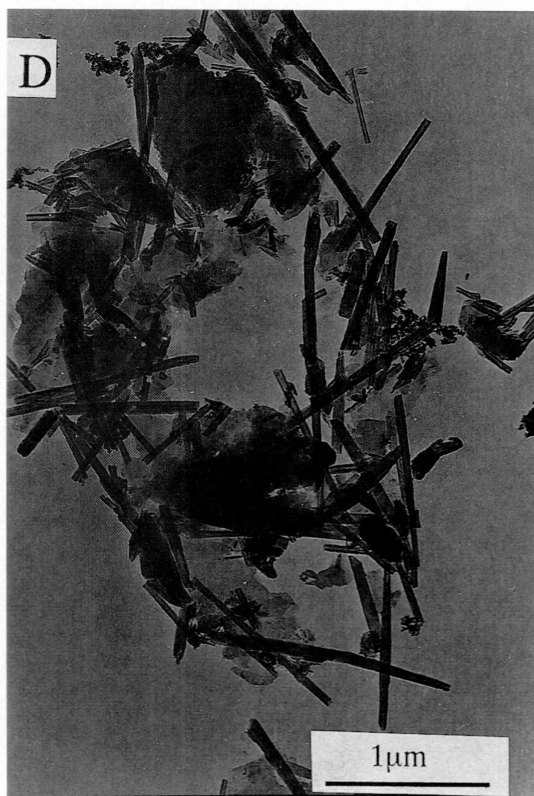
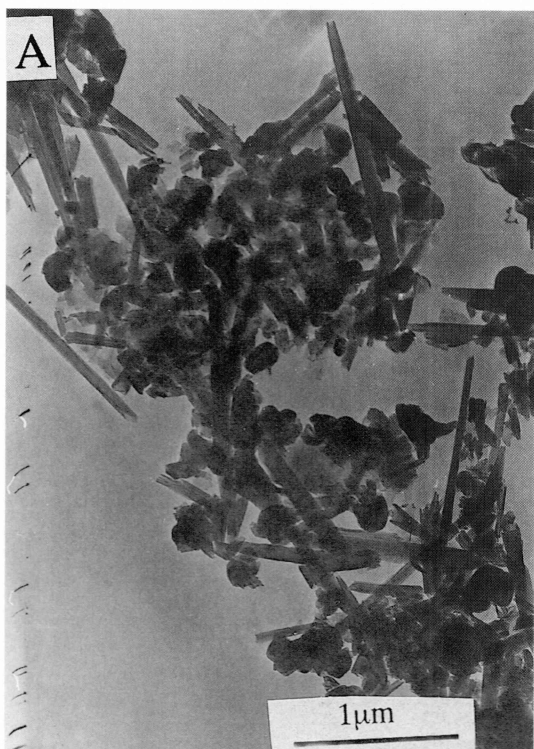


Plate 8

